UNIVERSITY OF GRONINGEN
UNIVERSITY MEDICAL CENTER GRONINGEN

Design of a Hardware Phantom for Digital Breast Tomosynthesis

Master Thesis

Author: Chikovskii Nikolai
Supervisors: Marcel Greuter and Alicja Daszczuk
Study Mentor: Bart Verkerke

Groningen
2015

Contents

Summary

This thesis presents a design concept of a prototype phantom used for both objective and subjective comparison of two breast imaging modalities: Digital Breast Tomosynthesis and Full-Field Digital Mammography. The main characteristic of the phantom is its modularity, so phantom compartments can be changed providing different properties for the single phantom, and enabling various investigation and calibration procedures of breast imaging equipment.
In Chapter 1, Analysis phase, the report discusses the problem of comparison of DBT and FFDM and provides information on state of the art phantoms used for both modalities. This section presents advantages and disadvantages of the phantoms, problem and goal description and definition, and stakeholder analysis, thus enabling the narrowing down of the design assignment and the forming of requirements and wishes for the designed phantom. The function analysis performed at this stage provided ground for the design characteristics for the preconcepts created during Synthesis phase.
Chapter 2 presents the early stage of the designing process, which includes generation of ideas for different design characteristics. Various solutions for each design characteristic were assembled into a morphological map with ten preconcepts. Of the ten preconcepts, only four were chosen for further evaluation according to the list of requirements and wishes. These four preconcepts were more thoroughly elaborated and then evaluated, and a list of their advantages and disadvantages assembled. Based on the evaluation of the four preconcepts, a final concept was selected. After the selection of the final concept, its composition and detailing are described. Drawings of all parts of the designed phantom are presented.
Chapter 3 discusses the prototyping stage of the project including: production of different versions of the prototype and their imaging using the mammography/DBT equipment of the Radiology department of the UMCG. The imaging results are presented and discussed in that section.
Chapter 4 presents manufacturing section providing information on the possible ways to manufacture the phantom in real life conditions; it describes methods and materials needed for phantom fabrication.
Failure Mode and Effect Analysis (0) discusses possible risks occurring during manufacturing and exploitation of the phantom. Identification of these risks may assist in their prevention.
Chapter 6 provides a review of possible future developments and improvements for the designed phantom.
The report concludes with Chapter 7, where societal impact of the project is explained and various ethical characteristics are presented.

Chapter 1. Analysis phase

Analysis phase is necessary to define the problem of the project, set the goals of the project, form design assignment. Next, a list of requirements and wishes is made to specify characteristics of the solution and narrow down possible ways of implementing it, consequent function analysis provides abstract perspective on the desired solution enabling wide range of possible design approaches.

Problem definition

Introduction

Human female breast consists of three types of tissue: fibroglandural, connective and adipose tissue. Fibroglandural tissue is the major component of dense breasts (where it composes more than 50% of breast volume), approximately 40% of women are estimated to have dense breasts and younger women have more widespread occurrence of dense breast. Breast density is one of the risk factors of breast cancer [1,2].

Breast cancer is globally the most frequently diagnosed invasive cancer in female population, approximately 1 out of 8 women in US will develop breast cancer in her lifetime [3]. Approximately 18% of all cancer cases accounted for breast cancer in Asia-Pacific region; breast cancer mortality accounted for 9% of all cancer-related deaths within the region [4].

Early identification of breast cancer is highly beneficial for successful treatment; therefore different techniques are present for cancer detection. The most currently used technique for cancer screening is using X-rays, and the standard X-ray modality is Full-Field Digital Mammography (FFDM). The image acquired by FFDM is a two-dimensional (2D) projection of the breast. Full-field digital mammography (FFDM) is used for women between 50 and 74 years old, screening is performed every 2 years [5]. Sensitivity of FFDM is inversely proportional to density of breast parenchyma (36% for “dense parenchyma” vs. 98% for “fatty parenchyma”). FFDM as a projection technique has lower sensitivity due to tissue superposition, which inhibits image quality leading to both false-positive and false-negatives [6]. Low sensitivity results in procedure risks being higher than benefits. MRI can be seen as an alternative; however, due to low specificity [7] it has higher number of false-positives and recall rates [8].

Another modality for X-ray breast imaging, which was recently introduced, is Digital Breast Tomosynthesis: the machine performs imaging over an arc of certain angle (which varies depending on the manufacturer), the reconstructed images present breast in slices forming a quasi-three-dimensional (3D) image. Due to such difference in image presentation DBT has theoretical advantage compared to FFDM in terms of superposition, since structures proximal to the X-ray tube of the machine should not obscure features of interest on the target level. There are data that DBT has higher sensitivity compared to mammography, however it is unclear whether it has increased interpretation over FFDM or not [9]. Given different levels of performance combining DBT and FFDM might be beneficial, and there are data on increased cancer detection [10,11]. Therefore, in order to assess advantages and disadvantages of both modalities, a comparison of their performance has to be made.

State-of-the-art phantoms

Standard procedure of assessing performance of mammography systems includes use of phantoms. During this procedure reference images are acquired and the system is calibrated to provide maximum image quality and recording sensitivity at the lowest possible radiation dose. Breast phantoms are designed to mimic attenuation of breast tissues, simulate breast structure and assess various objective image quality parameters. The phantoms must provide enough potential for image quality (IQ) and dose optimization.

To our knowledge, there exists no standard phantom which can be used for the comparison of FFDM and DBT modalities. Brunner et al. [12] performed image quality evaluation in DBT with

four state-of-the-art breast phantoms which included: CIRS BR3D phantom, ACR Prototype FFDM Accreditation phantom, Penn anthropomorphic phantom, and Quart mam/digi EPQC phantom.

Figure 1. Phantoms investigated by Brunner et al. [12]: a – CIRS BR3D phantom [13]; b – ACR Prototype FFDM Accreditation phantom [14]; c – Penn anthropomorphic phantom [15]; d – Quart mam/digi EPQC phantom [16]

- CIRS BR3D phantom

CIRS BR3D is a flat semicircular phantom consisting of 6 slabs made of materials 100% equivalent to adipose and glandular tissues; these materials are "swirled" together in 50/50 ratio by weight. One of the slabs, marked as a target slab contains various objects for image quality evaluations, such as microcalcifications, fibrils and masses [13].

- ACR Prototype FFDM Accreditation Phantom

This phantom is based on a CIRS Model 015 phantom with a size in the range of the detector size. It consists of a PMMA block with homogeneous wax insert inside the block. The phantom allows for the calculation of noise properties and contains a cavity to calculate the contrast-to-noise ratio (CNR).

- Penn anthropomorphic phantom

A prototype phantom developed at the University of Pennsylvania, with the special purpose of 3D X-ray imaging. First, a computer model was made which simulated breast anatomy with different structures within, such as adipose and glandular compartments, Cooper's ligaments and skin. The phantom was manufactured on the basis of the computer model and it consists of several slabs. The resulting images are within the grayscale range of real breast tissues. An additional slab can be used for contrast enhanced digital breast tomosynthesis.

- Quart mam/digi EPQC phantom

  This phantom consists of a PMMA block with 12-step wedge for simulation of various breast densities. Each step contains low-contrast number indicating the PMMA thickness corresponding to the step. Titanium strip dividing each step allows calculation of the CNR for various thicknesses. Brass and lead squares are located inside the phantom; their edges can be used for Modulation Transfer Function (MTF) calculation. The phantom also contains: Landolt rings for subjective image quality evaluation and a slot for a dosimeter detector

After performing DBT screening with these phantoms, their advantages and disadvantages were discussed and presented in Table 1:

Table 1: Advantages and disadvantages of the phantoms reviewed in the study of Brunner et al. [12]

Phantom	Advantages	Disadvantages
CIRS BR3D	• Qualitative evaluation of reconstructed slice images	• No features for objective image quality evaluation • Impossible to analyze reconstruction depth • Results depend on the order of slabs
ACR Prototype FFDM	• Objective evaluation of noise variance and CNR	• Impossible to analyze reconstruction depth • Low number of features for diverse IQ assessment
Penn anthropomorphic	• Breast anatomy imitation • Slot for dose assessment • Enables contrast enhanced DBT	• No features for objective image quality evaluation • Limited quantitative evaluation capability
Quart mam/digi EPQC	• Features for objective evaluation of MTF, NPS or CNR	• Limited capabilities for objective and subjective quality evaluation • Does not resemble real breast anatomy

All these phantoms were initially designed for FFDM (except for Quart phantom which was also designed for DBT). According to the study of Brunner, none of them can be used for adequate DBT quality evaluation as they lack complete set of features for proper DBT evaluation, such as in plane distance accuracy, slice sensitivity profiles, etc.

Three out of the four phantoms investigated in the aforementioned study are based on the principle of 2D projection of the breast, and their composition resembles 2D arrangement of tissues or none at all. Only the Penn phantom mimics the 3D arrangement of breast tissues.

Additional analysis of other state-of-the-art phantoms shows that all of them are designed under the condition that breast consists of 50% adipose tissue and 50% glandular tissue [12]. A study of Yaffe et al. [17] provides new information on breast composition discrediting the myth of breast consisting of 50% adipose and 50% fibro-glandular tissue. This myth was formed due to misinterpretation of 2D projection of 3D distribution of breast tissues. However, the study of Yaffe et al. showed that real percentage of fibro-glandular tissue is much lower and for majority of women population is lower than 45 %. Thus future versions of the phantoms should allow for variation of density and not simplify the breast structure by using the 50/50 approach.

Conclusion: Problem definition

The study of Brunner et al. together with other information on the current development in mammography phantoms, enables identification of the following problems of comparison FFDM and DBT modalities:

1. No comparison of FFDM and DBT modalities was performed using single technique or equipment
2. No current phantom can be used for a complete (including both objective and subjective) comparison of FFDM and DBT
3. Most current phantom designs are based on a wrong 2D perception of breast composition, which is due to characteristics of previously used imaging modalities; this concept cannot be used for a (quasi-)3D imaging modality (e.g. DBT)
4. Most current phantoms (which mimic breast architecture) provide only a single set of features for variation of breast parameters, andtheir design lacks the option to vary the density of simulated breast parenchyma

All these points can be assembled into a problem diagram presented in Figure 2.

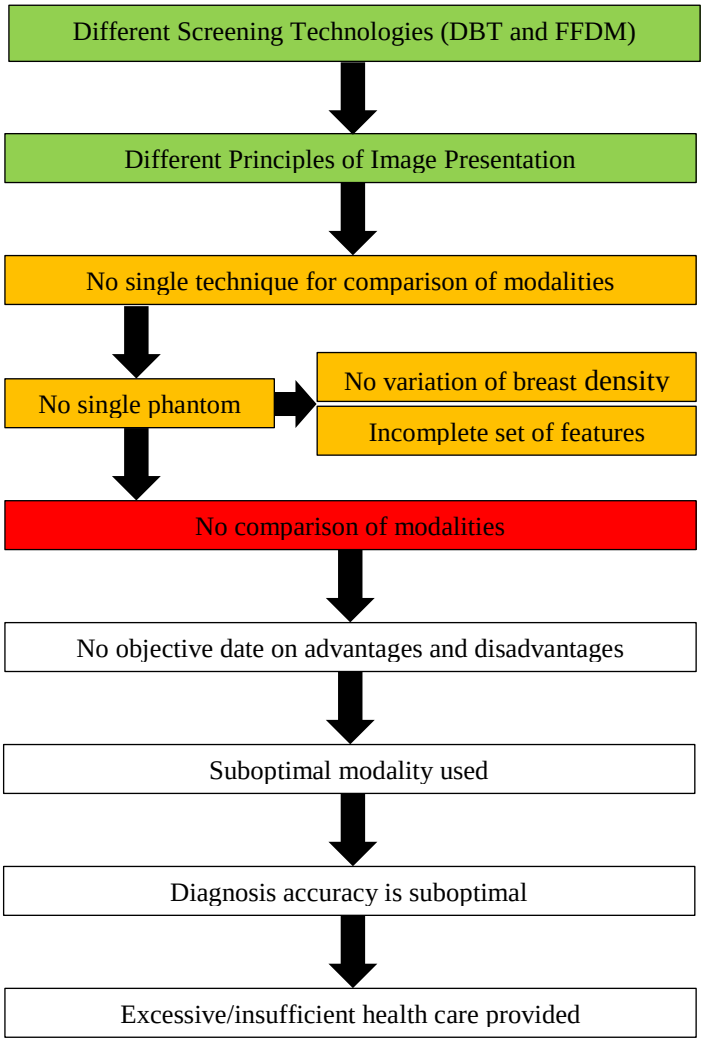

Figure 2: Problem diagram

DBT and FFDM have different image representation principles, resulting in necessity of comparison to identify advantages and disadvantages of both modalities. As long as the problem of absence of a proper comparison method persists a suboptimal imaging modality is used for breast cancer identification resulting in suboptimal diagnosis accuracy; in connection with that patients might undergo excessive or insufficient treatment.

Stakeholders

Analysis of stakeholders provides information on involvement of different target and associated groups into the project with consequent potentials and deficiencies arising from it.

Table 2: Stakeholders

Stakeholder	Characteristics	Expectations	Potentials and deficiencies	Implications and conclusions for the project
Radiologist	Diagnoses patients; decision affected by technology	Desires equipment that provides better diagnostic accuracy	Feedback on performance of the phantom; may assist in clinical trial of the phantom; subjective on performance of the new design; conservative due to success in using previous phantoms	It may take time to convince the medical professional to use the phantom; also the best performing modality might be disliked by the professional due to previous experience
Technician	Provides technical support of radiological equipment	Easy and objective comparison procedure; possibility of additional adjustment	On-place technical specialist, can make mistake in comparison procedure	Technician should be educated to properly work with the phantom; Technician can provide feedback regarding technical characteristics of the phantom
Researcher/ Scientist	Performs scientific research and assessment of the designed solution	Strives for quantified data on performance assessment; new solution might provide new scientific ideas	Objective on performance of the phantom; might be biased by preferred manufacturer or technology	May provide scientific justification of phantom performance and suggest new ways to solve the arising problems
Engineer	Designs a technical solution to the problem	Desires to develop a solution superior to already present in clinic	Technology driven; lacks user knowledge	Engineer designs the phantom by simplifying the real life situation; should be consulted by scientific and medical professional to ensure high quality of the design; can improve future version of the phantom
Manufacturer	Fabricates designed object	Wishes to use more cost-efficient technology compared to current benchmark	Cost-effectiveness may reduce performance; Production defects may affect procedure results	Can provide new data on manufacturing procedures, reducing the costs while preserving the quality; should be controlled by an engineer to provide certain level of quality
Patient	Screened by possibly-suboptimal modality	Expects better healthcare	Unique cases may complicate comparison results due to inability to account for all variations of breast structure in single design	Patients can be asked to anonymously provide data for verification of performance of the phantom

Goal Description

The goal of this project is to resolve the problem of comparing DBT and FFDM imaging modalities. The solution can be – a design of a single phantom used for both DBT and FFDM modalities. The Figure 3 shows the effect of introducing a new phantom for this purpose.

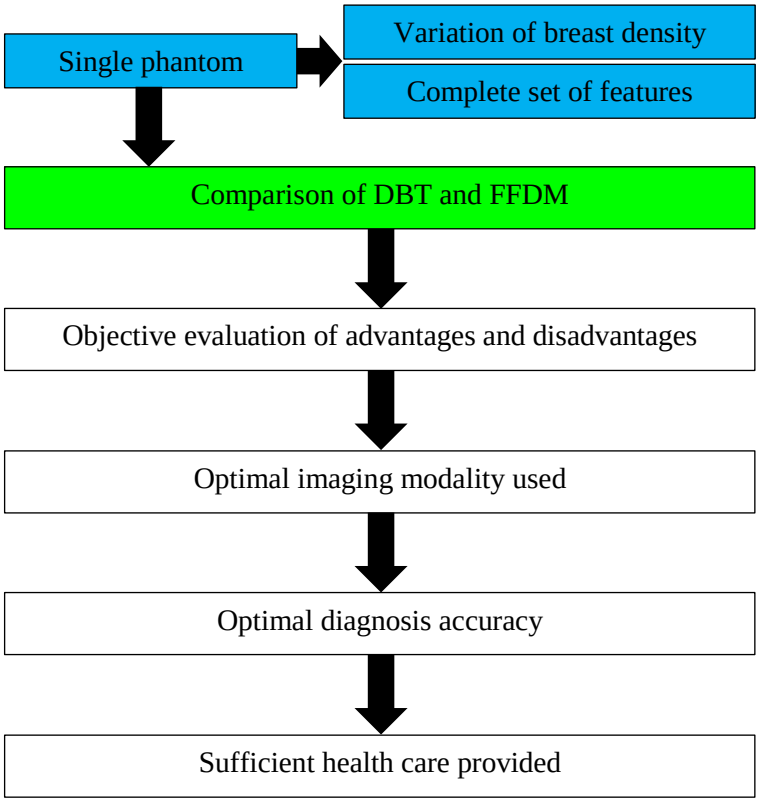

Figure 3: Goal diagram of the project

The goals of the project can be defined as follows:

- The designed phantom must provide ability for comparison of DBT and FFDM modalities
- The designed phantom must provide the means for variation of simulated breast density
- The designed phantom must provide the possibility for implementation of features for both subjective and objective evaluation of image quality i.e. modality performance

Design Assignment

Given these goals a design project assignment was formulated:
Develop a concept of a phantom for the comparison Digital Breast Tomosynthesis and Full-Field Digital Mammography modalities; the phantom design should enable variation of the simulated breast density and the implementation of features for image quality evaluation.
Therefore, during the project the following tasks must be addressed and completed:

- The concept of the phantom must be developed and detailed for further manufacturing
- The manufacturing of the phantom must be described
- A prototype of the phantom must be produced
- Initial comparison of modalities using the prototype must be performed

Demarcations

Time limitations imposed on the project resulted in certain restraints on the designing of the phantom for the comparison of DBT and FFDM.
First demarcation is that only a general concept of the modular phantom would be designed, i.e.:

- No additional investigation and elaboration of such phantom features as realistic breast anatomy (actual shapes and dimensions of breast structures and components)
- No means for providing these features would be developed (e.g. algorithms for generation of breast anatomy, etc.)
- The project includes only development of the general composition of the phantom, materials and features necessary for the production of the initial experimental phantom
- Further work might be necessary for the development of the concept into complete solution for healthcare industry

Second demarcation involves manufacturing of the phantom:

- No real life phantom would be produced, only a "proof of concept" prototype
- The prototype will provide the evidence that the presented design suffices the requirements and wishes imposed to the project, and feasibility of the phantom manufacturing
- Manufacturing of the phantom would be described in the report with all the materials and methods necessary for the final fabrication of the phantom

Requirements and Wishes

In order to narrow down the range of possible solutions and make them as objectively oriented as possible, certain requirements and wishes are necessary to be defined.

Requirements

Requirements form the essential characteristics of the future design. These parameters are later evaluated for each preconcept to decide on what preconcept to elaborate into the final design. The requirements for the phantom are presented below:

- Design and performance requirements
    - Must have modular design
    - Must include masses of different shapes, size and contrast, which are subjected to superposition by other structures
    - Phantom must enable variation of densities and patterns of breast parenchyma
    - Phantom must be made of materials with X-ray attenuation and scattering characteristics mimicking those of breast tissue and different breast lesions, malformations and microcalcifications. Phantom must allow for inclusion of features for subjective and objective image quality evaluation, such as:
        - Landoldt rings
        - Resolution lines
        - Spatial resolution
        - MTF
        - CNR
    - Must withstand compressive forces applied by fixating plates of mammography machines (ca. 150 N)
- Ergonomics requirements
    - Phantom must match the sizes of commercial phantoms used for a routine mammography calibration procedure
    - Phantom components must be interchangeable and enable easy assembling and disassembling

Wishes

Wishes are the desired characteristics of the design object, they are not essential but may play a definitive role when several preconcepts have similar evaluation grade. The wishes towards the phantom design are:

- Phantom should be producible by means of 3D printing
- Phantom should have slots for dose measuring devices
- Phantom should include a component which can be also used as a shell for the phantom

Function Analysis

Function analysis is performed to generalize the structure of the designed phantom. Generalization provides bigger range of ideas suitable for
Store Material (some components of the phantoms must contain other components and features of the phantom)

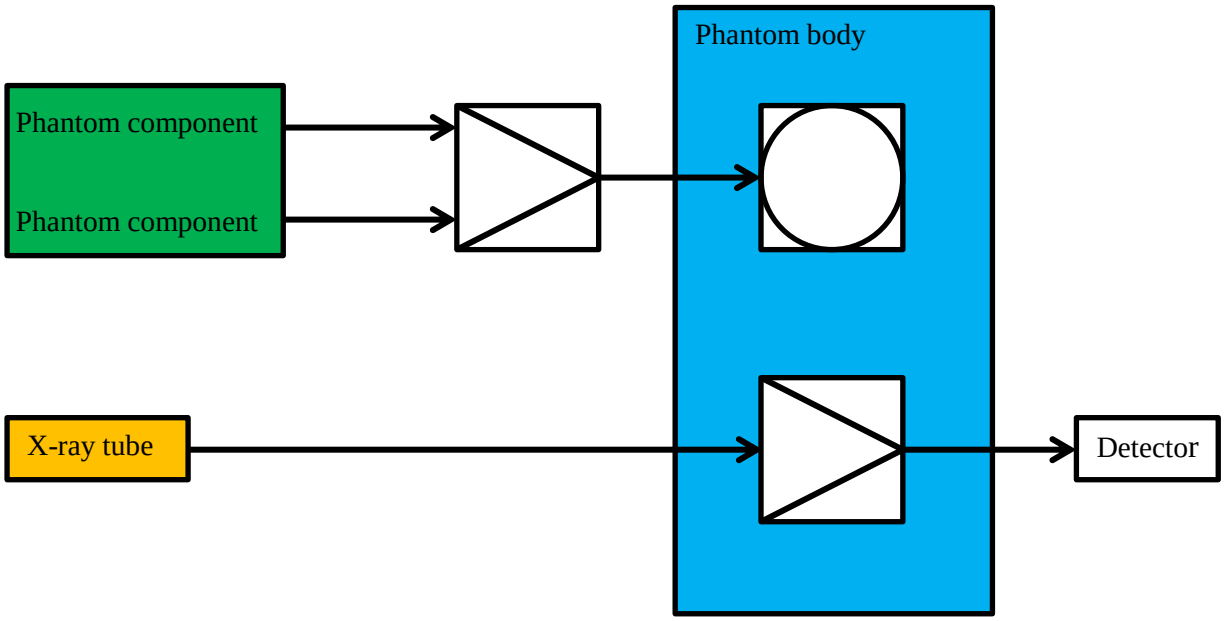

Figure 4: Function diagram

Legend

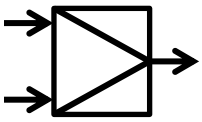

Connect Material - components of the phantom must be easily assembled into single body

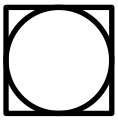

Store material - some components of the phantoms must contain other components and features of the phantom

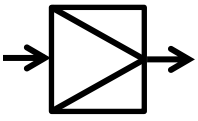

Transform Energy - materials used for the production of the phantom must properly attenuate incident X-ray radiation to produce images

Chapter 2. Synthesis phase

In the synthesis phase the solution for the problem outlined in the analysis phase is elaborated in more details. Results of the function analysis were used for definition of design characteristics of future preconcepts. Next, ten preconcepts were formed and presented by a morphological map of their characteristics. Only four preconcepts were chosen for further more detailed elaboration and evaluation according to requirements and wishes leading to a final concept. The detalisation of the final concept was performed afterwards, all components described and both their 3D models and drawings presented.

Design Characteristics

After applying the function analysis to the design procedure specific design characteristics can be defined for each function:

Store material – the shape of the phantom body will affect the resulting image. Therefore, it must be either anthropomorphic or reasonably (quantitatively justified) close to it.
Phantoms with different deformability might pose an additional interest for investigation because they simulate breast compression, thus two different types of the phantom are introduced: hard phantom, which has constant shape, and soft compressible phantom.

- Shape of the phantom
  - Simplified
  - Anthropomorphic

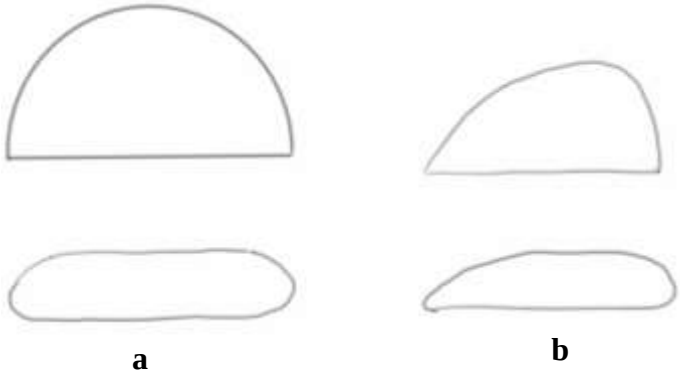

Figure 5: Shape of the phantom: *a* – simplified, *b* - anthropomorphic

- Compressibility
  - Hard phantom – constant shape
  - Soft phantom – compressed during screening procedures

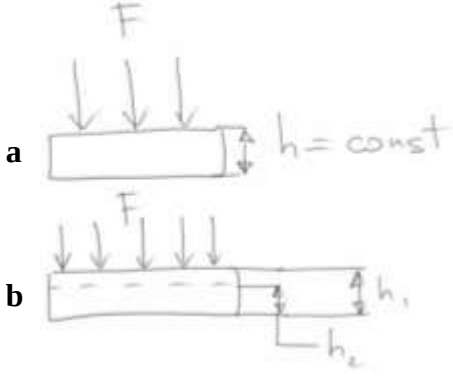

Figure 6: Compressibility of the phantom: *a* – hard phantom, *b* – soft phantom

Connect Material – in order to implement the requirements of modular design and variable breast density the phantom must consist of several components. Phantom structure can be

implemented in three different ways: concentric layered structure, "pincushion" structure, and slab structure:

- Structure
  - Concentric layered
  - Pincushion
  - Slabs

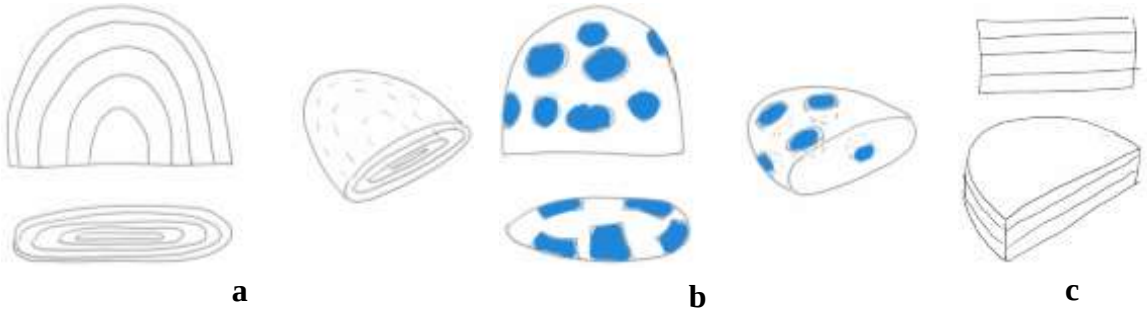

Figure 7: Structure of the phantom: *a* – concentric layered, *b* – "pincushion", *c* - slab

Transform energy – by attenuating the incident X-rays, the phantom lowers the beam energy in a manner similar to the natural human tissue. By choosing and properly positioning tissue-equivalent materials a realistic image can be achieved. The components of the phantom can be individually manufactured in a homogeneous or a heterogeneous manner; and the latter can be subdivided into anthropomorphic and non-anthropomorphic implementation:

- Composition (distribution of different materials in each element of the phantom)
  - Homogeneous – single material in each element
  - Heterogeneous – different materials present in each element
    - Anthropomorphic
    - Non-anthropomorphic

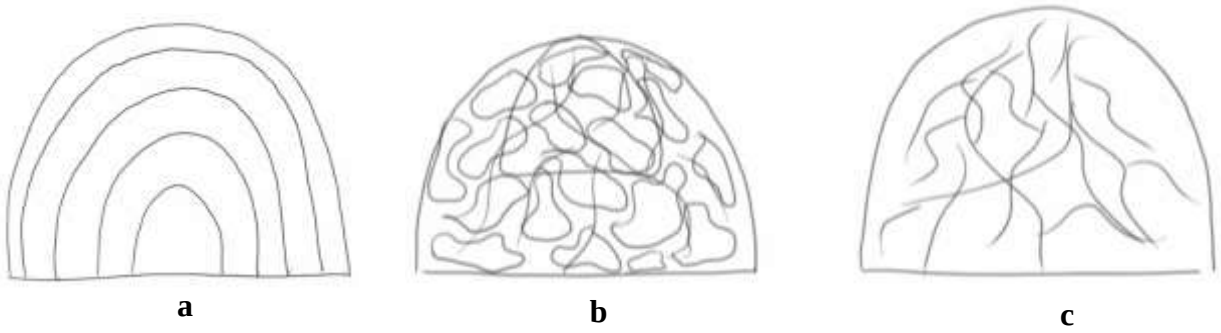

Figure 8: Composition of the phantom: *a* – homogeneous, *b* – heterogeneous anthropomorphic, *c* – heterogeneous non-anthropomorphic

Using the aforementioned functions and design characteristics implied by them a morphological map can be formed (Table 3). This map presents ten preconcepts, and the variants of function and design characteristic implementation are listed for each preconcept.

Table 3: Morphological map

Function	Design characteristic	PC 1	PC 2	PC 3	PC 4	PC 5	PC 6	PC 7	PC 8	PC 9	PC 10
Store material	Shape	Non-anthropomorphic	Non-anthropomorphic	Non-anthropomorphic	Anthropomorphic	Anthropomorphic	Anthropomorphic	Non-anthropomorphic	Anthropomorphic	Non-anthropomorphic	Anthropomoprhic
	Compressibility	Hard	Hard	Hard	Hard	Hard	Hard	Soft	Soft	Soft	Soft
Connect material	Structure	Concentric	Pincushion	Slabs	Concentric	Pincushion	Concentric	Concentric	Concentric	Pincushion	Pincushion
Transform energy	Composition	Heterogeneous, non-anthropomorphic	Heterogeneous, non-anthropomorphic	Heterogeneous, non-anthropomorphic	Heterogeneous, anthropomorphic	Heterogeneous, anthropomorphic	Homogeneous	Heterogeneous, non-anthropomorphic	Heterogeneous, anthropomorhic	Heterogeneous, Non-anthropomorphic	Heterogeneous, anthropomoprhic

Four Preconcepts

Out of the ten preconcepts four were selected for further more detailed elaboration and evaluation to find the final concept. Preselection of four preconcepts is due to similarity of other concepts in their hard implementation given the time limitations of the project and information available at the moment.

Preconcept 1

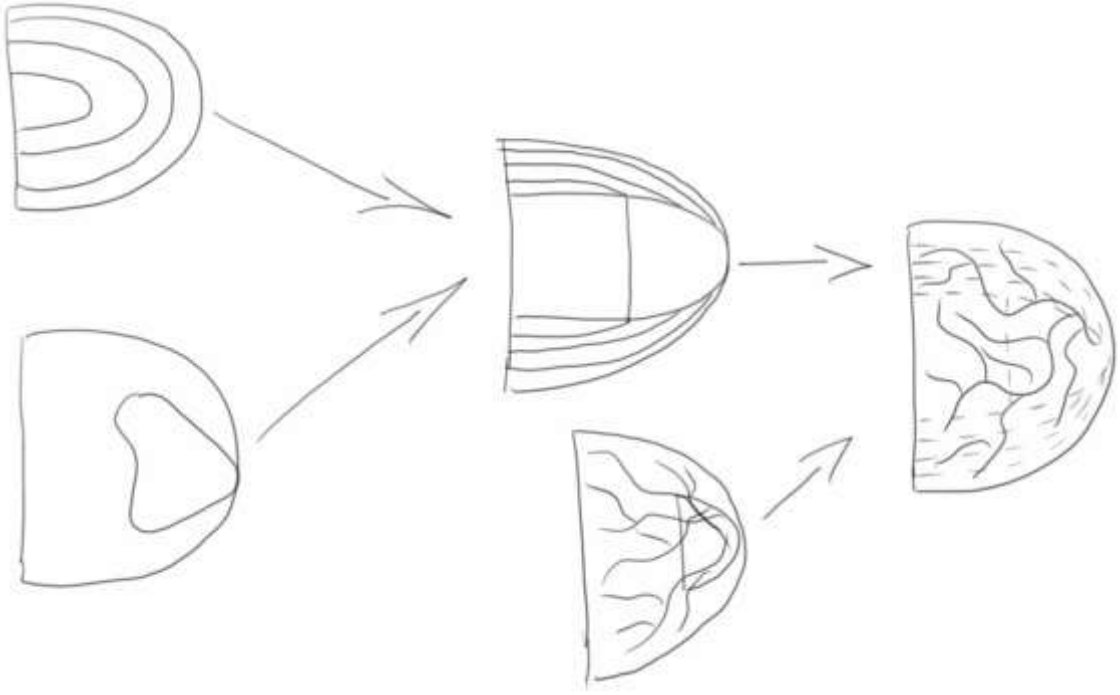

Figure 9: Development of the preconcept 1

The phantom consists of several concentric components; each of them mimics a layer of the breast tissue (Figure 9). The layers go from exterior to interior in the following order:

- Skin layer

This layer will mimic the skin covering the breast. It will also serve as a shell for the phantom therefore this layer will be the only constant component of the phantom.

- Several adipose layers

Next several "adipose" layers are forming the bulk of the phantom. These layers will have different variants of tissue mimicking patterns and breast densities. Various features (e.g. Landoldt rings, cubes, spheres, etc.) can be embedded into the "adipose" layers.

- Fibro-glandular region

Last and the most internal component of the phantom will mimic the fibro-glandular region (FGR) of the breast. It will consist of two parts:

  - Outer shell to provide proper installation within the complex phantom structure; shape of this shell will be uniform for all variant of FGR
  - Inner compartment, which can have variable shape and volume. This compartment might also include various features for assessing modality performance (e.g. CNR, MTF, etc.).

Preconcept 2

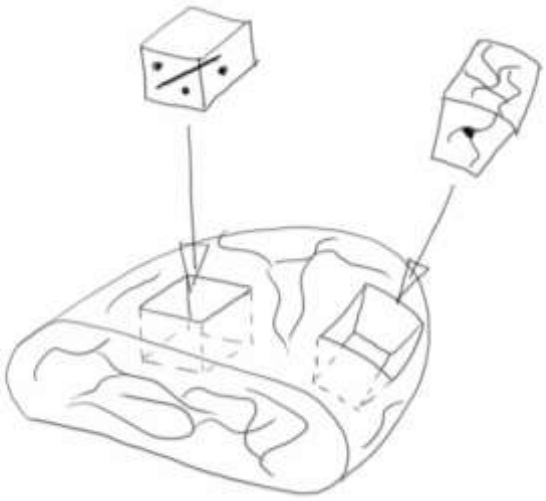

Figure 10: "Pincushion" phantom with different insertions: one containing features and one with simulation of breast structure

The preconcept is based on the structure of a pincushion (Figure 10). The bulk of the phantom is a "cushion" with certain internal structure which remains constant. The phantom also has a number of slots where various insertions ("needles") can be installed. These "needles" will change phantom density and composition; they also can have different embedded assessment features, dosimeters, etc.

Preconcept 3

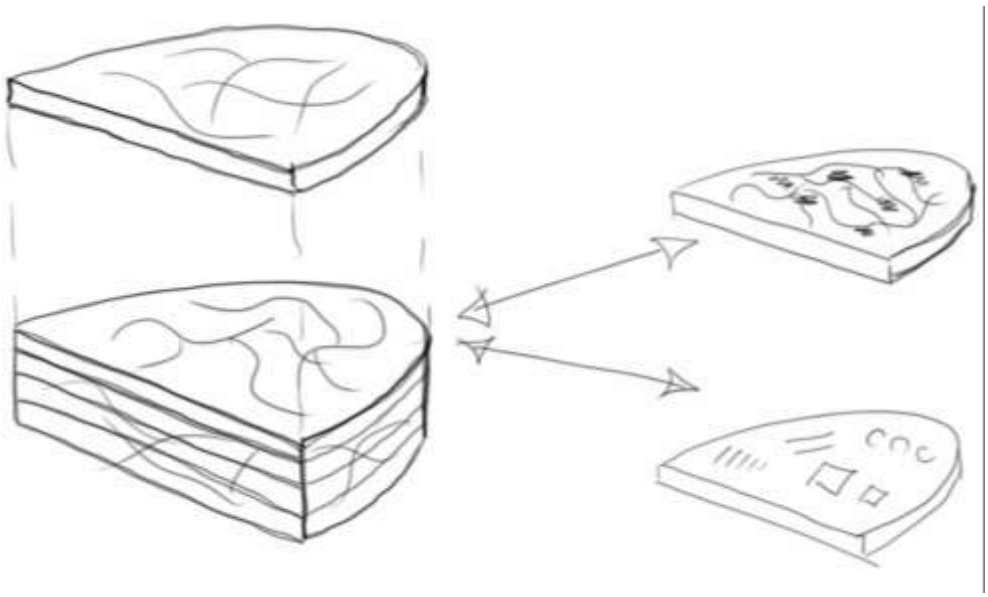

Figure 11: A phantom with slab structure: slabs can contain features or simulation of breast structures

The phantom is implemented using the widely applied approach of slab division (Figure 11). Each slab represents a set of slices of the breast. Breast composition can be varied by changing the slabs. Besides breast tissue mimicking patterns the slabs can also include various features and objects for the evaluation of phantom performance.

Preconcept 4 (7)

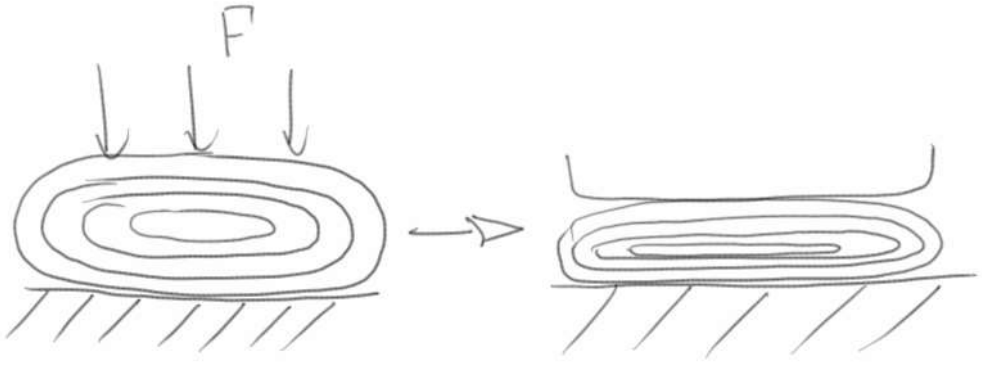

Figure 12: Compressible phantom

This preconcept shares the idea and structure of the Preconcept 1. However for this variant soft compressible materials are used (Figure 12). The phantom can put into breast imaging machine, where it would be consequently fixed by compression, thus simulating the breast compression and providing additional variation of breast tissue patterns.
Next, a list of advantages and disadvantages of each preconcepts (Table 4) was compiled before the evaluation and the choice of the final concept (Table 5).

Table 4: Advantages and disadvantages of preconcepts

Preconcept	Advantages	Disadvantages
Preconcept 1	• High modularity • Durable • Different manufacturing techniques applicable • High variability of breast representation	• To change one component disassembling the whole phantom might be necessary • No compression option • Big number of switchable components
Preconcept 2	• Easy to switch components	• Low variability of breast representation • No compression option • Single bulk body
Preconcept 3	• Simple production	• Low variability of breast representation • Low modularity • Extra alignment is necessary • No compression option
Preconcept 4	• Compression option • High modularity • High variability of breast representation	• Big number of switchable components • To change one component disassembling the whole phantom might be necessary • Few variants of manufacturing • Not durable in cycles of repeated compression • Pairs of different materials might result in cracks and deformities

Table 5: Evaluation of preconcepts

Requirements	Preconcept 1	Preconcept 2	Preconcept 3	Preconcept 7
Modular design	5	3	2	4
Withstand fixating forces	5	5	5	3
Made of materials mimicking X-ray properties of real breast tissues	5	5	5	3
Presence of different structures mimicking breast composition	5	4	4	5
Capacity for installing features used for assessment of modality performance	4	5	5	4
Variation of breast parenchyma density	5	3	2	5
Matches the dimensions of standardly used phantoms	5	5	5	4
Shape quantitatively justified	4	4	4	5
Total	38	34	32	33

Besides evaluation of the preconcepts according to the requirements (Table 5) the **Preconcept 1** was selected as the final concept because it has the following characteristics:

- It enables easy implementation of modular structure
- It allows for high number of breast structure patterns
- Big number of manufacturing techniques
- Its structure makes it durable to external mechanical impacts

All these advantages outweigh the disadvantages presented in Table 4.

Final Concept

This section describes the general composition of the final concept of the phantom and provides detailed information on the design of the phantom and its component together with explanation on how different versions of the components and additional features can be implemented within the design.

General shape and composition of the phantom

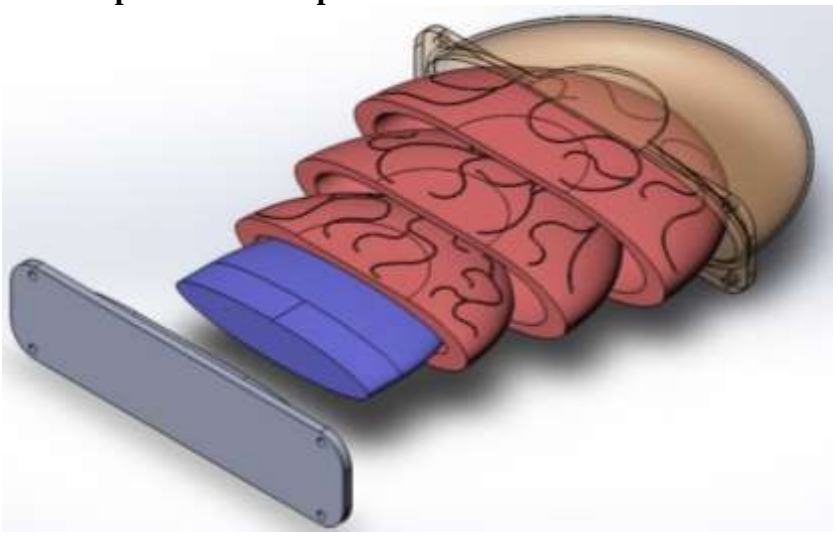

Figure 13. Exploded view of the phantom

D-shape of the phantom was selected to resemble the average shape of a compressed breast during mammography procedure. A study on the shapes of compressed breasts was performed by Feng et al. [18], where principal component analysis was used to objectify compressed breast shapes during mammography. In this study average PCA models were derived allowing for the determination of certain geometric dimensions and shape of the phantom; it was concluded that semicircular profile of the breast is one of the most widespread during compression for mammography.

Dimensions of the phantom are presented in Figure 14. The thickness of the phantom was chosen similar to standard phantoms used for mammography 50 mm, and the radius of the phantom was set to 100 mm.

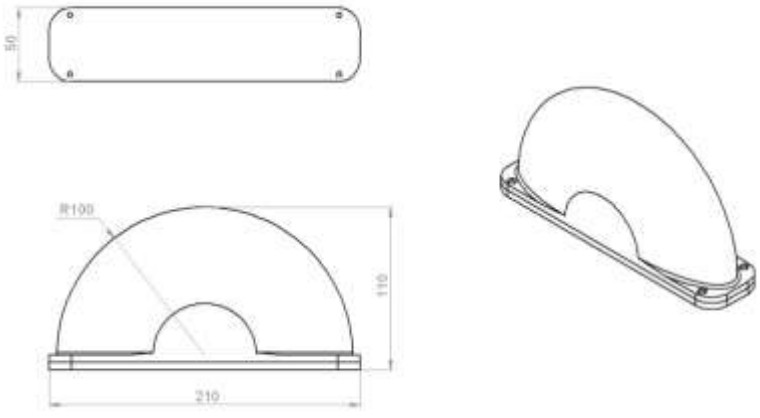

Figure 14: Assembled phantom

Structure

Skin

The skin component is the only constant part of the phantom; it is used to simulate skin tissue, keep and preserve the whole assembly. The thickness of the skin compartment is set to 2 mm and it lies within the range of normal skin thickness [19].

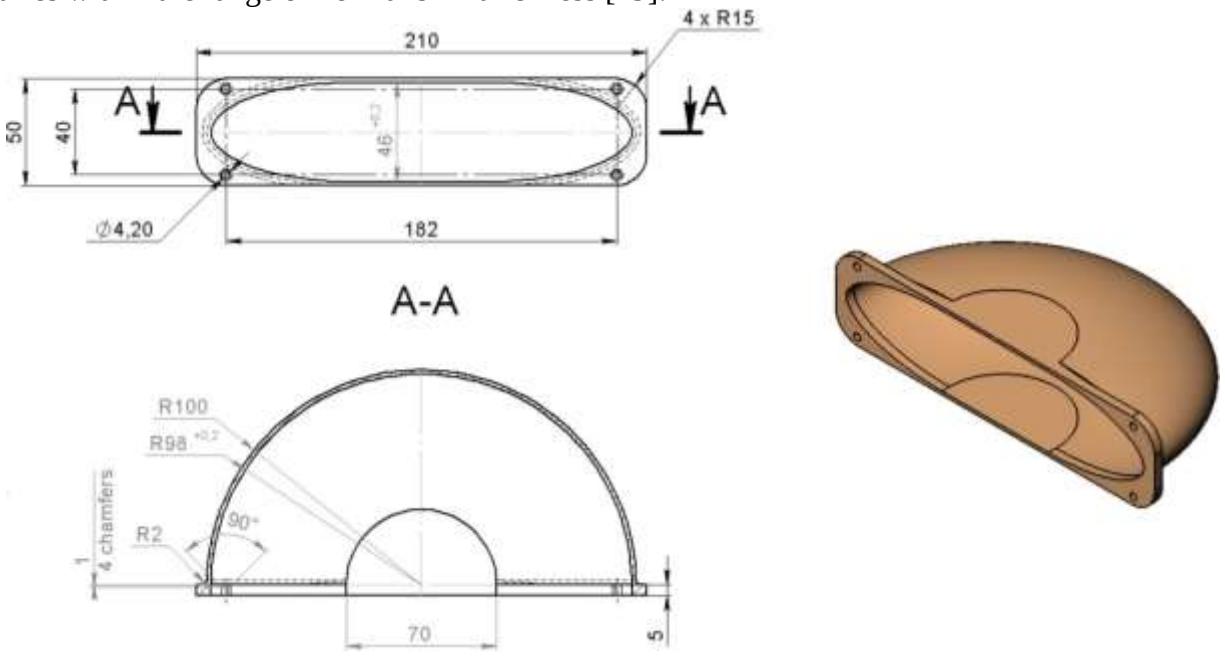

Figure 15: Technical drawing of the skin component

The back cover component (Figure 16Figure 16: Technical drawing of the) together with the skin component forms a complete shell, which encloses and protects other components of the phantom.

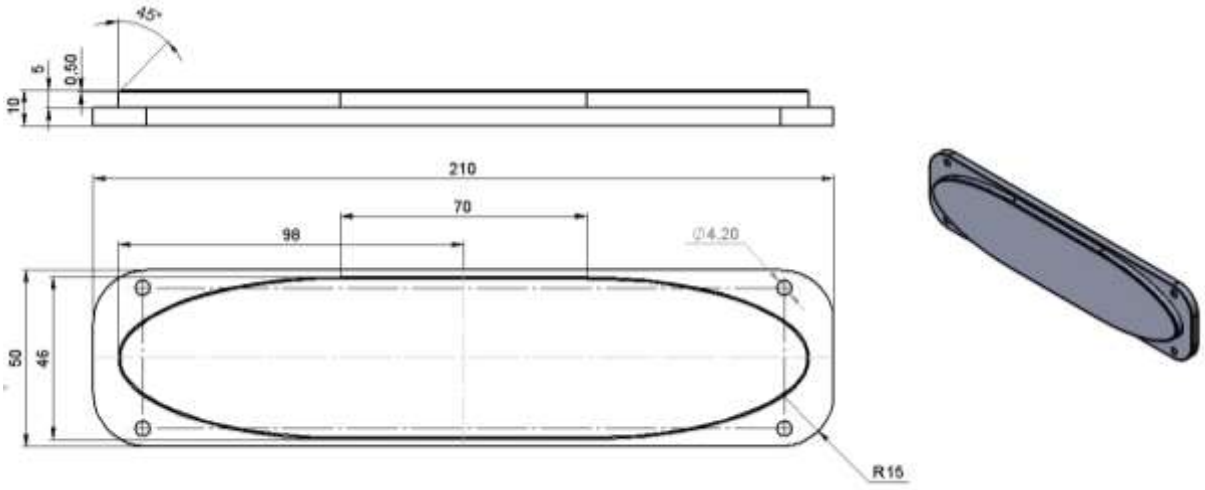

Figure 16: Technical drawing of the back cover of the phantom

Adipose layers

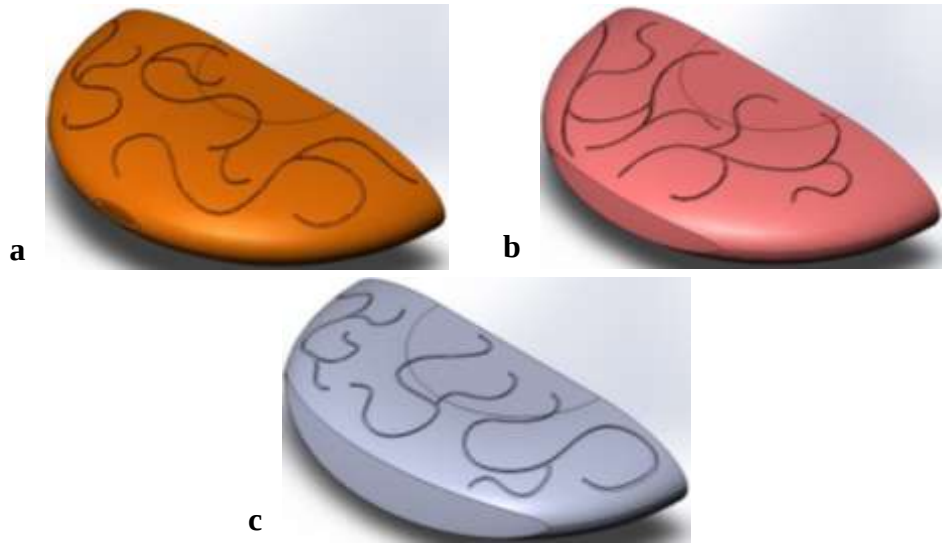

Figure 17: Adipose layers: *a* – 1st adipose layer; *b* – 2ns adipose layer; *c* – 3rd adipose layer

These components are called "adipose" layers because they simulate the part of the breast, which mostly consists of adipose tissue, while also enabling simulation of fibro-glandular components. Adipose layers form the bulk of the phantom.
The layers are designated as follows (Figure 18):

- 1st layer – outer layer
- 2nd layer – middle layer
- 3rd layer – internal layer next to fibro-glandular component

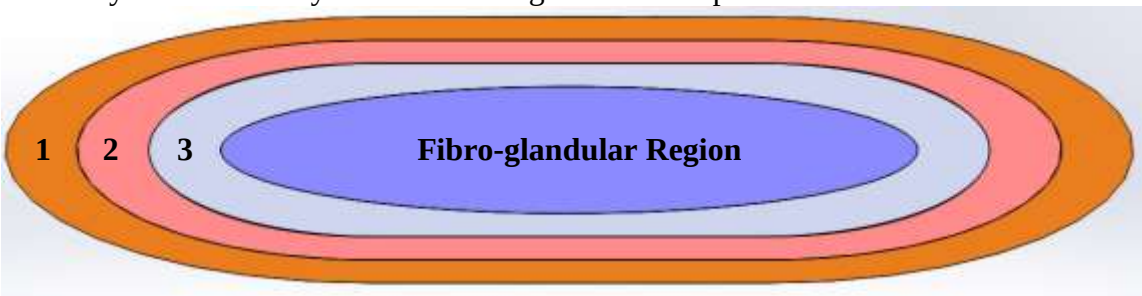

Figure 18: Rear view of the adipose layers alignment

In the initial version of the phantom, fibro-glandular structures are simulated by grooves on the external surface of the layers, these grooves are later filled with an epoxy based resin with attenuation and scattering parameters similar to real glandular tissue, thus mimicking the superposition of different structures within a breast.
The design of the "adipose" layers implies further improvement in terms of mimicking the glandular structures. In the next versions the grooves can be replaced by a more complex structure, which can be designed by software means to completely resemble real breast architecture.
Additional interchangeable layers can be used to provide even more detailed evaluation of modality performance, such as:

- Resolution
- Modular transfer function (both 2D and 3D)
- Contrast-to-noise ratio
- Artefact detection
- Missed tissue

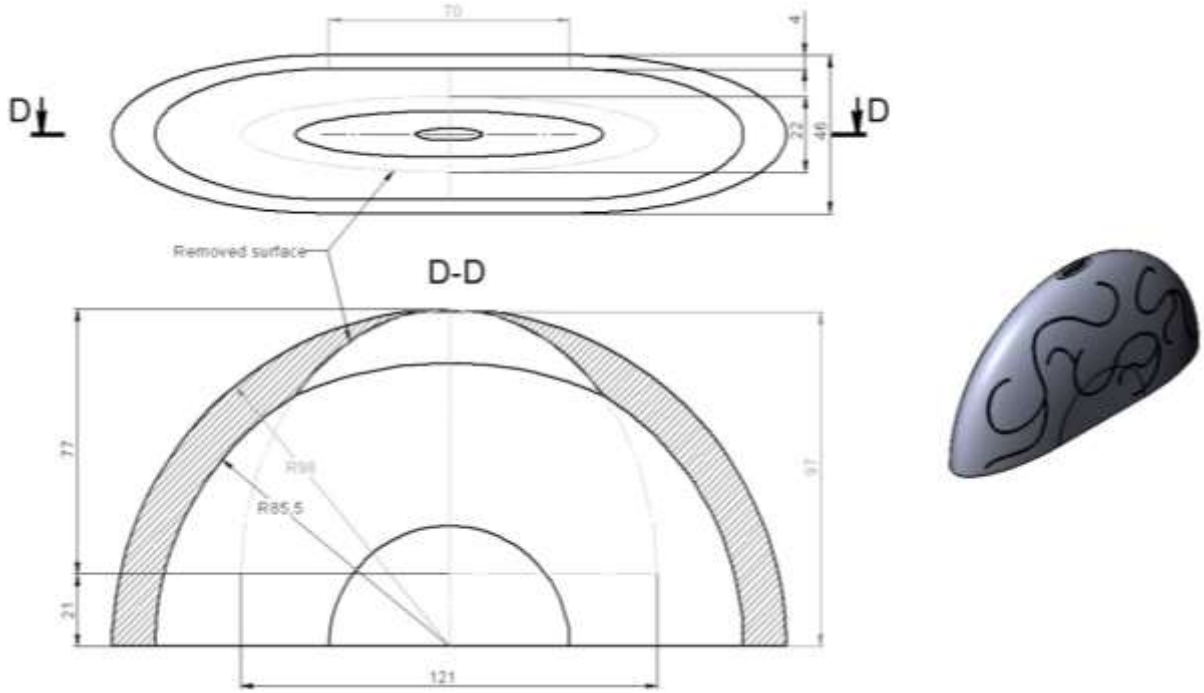

Figure 19: Technical drawing of the 1st adipose layer

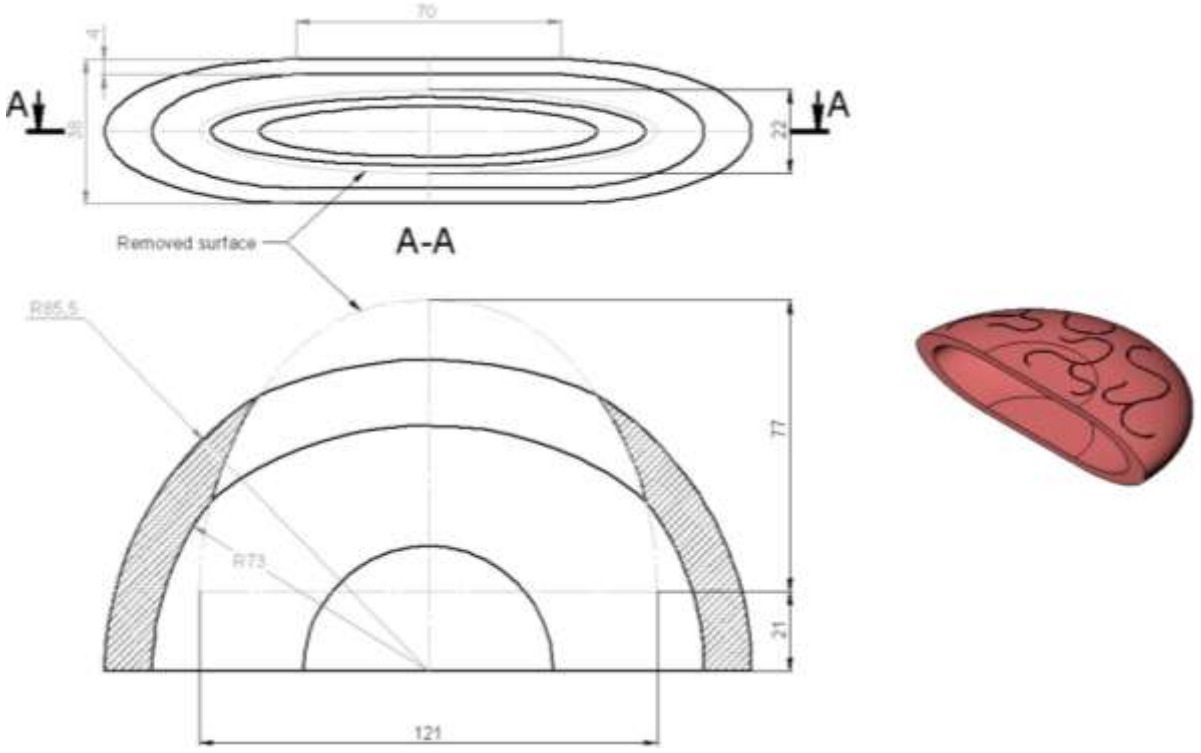

Figure 20: Technical drawing of the 2nd adipose layer

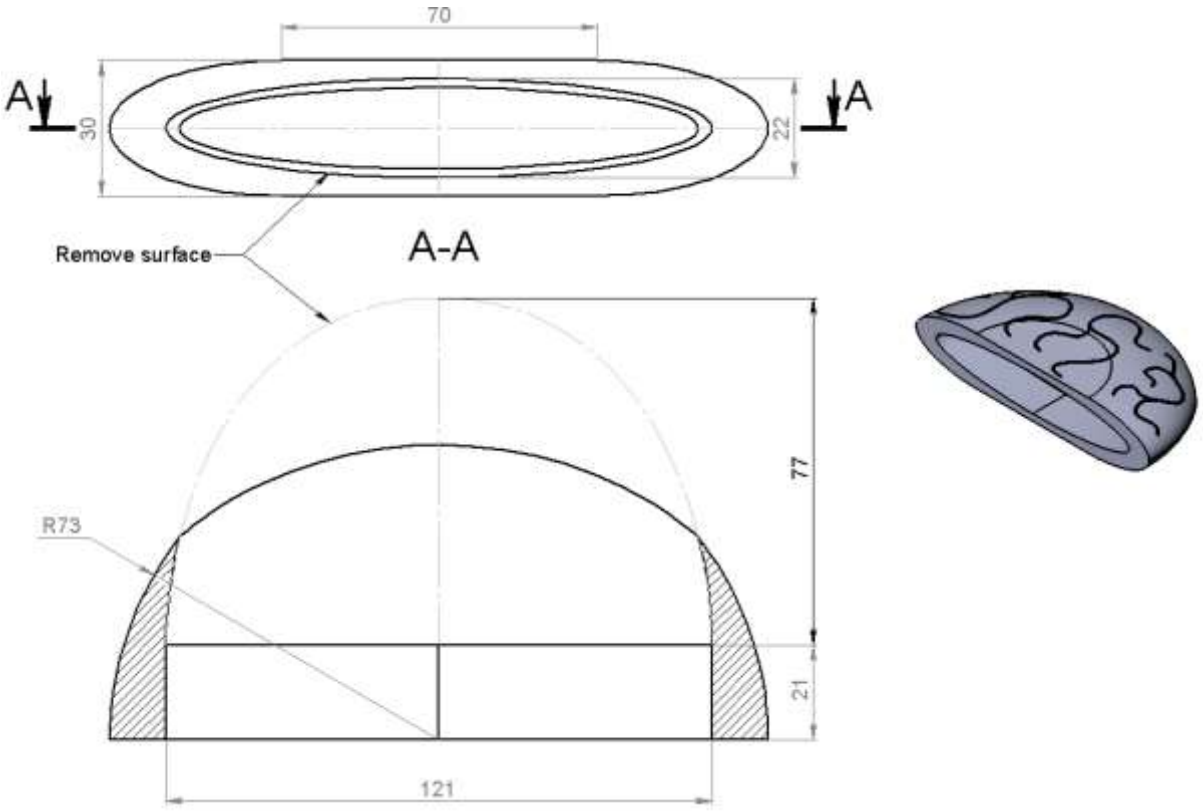

Figure 21: Technical drawing of the 3rd adipose layer

Fibro-glandular region

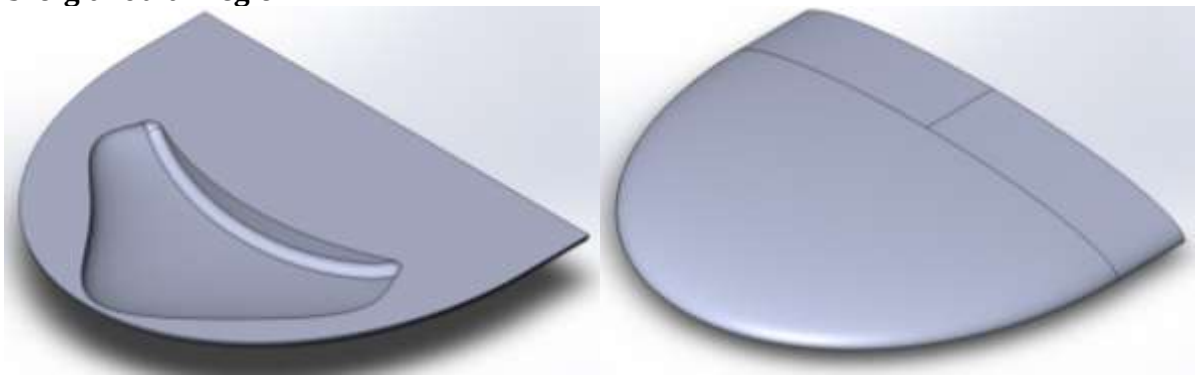

Figure 22: Fibro-glandular region component

Fibro-glandular region (FGR) component represents the most internal part of the breast – the fibro-glandular structure composed of mammal lobuli and lactiferous ducts (Figure 22).
The FGR component can have two versions:

- Whole component (Figure 23)
  The component is a single body made of a material mimicking glandular tissue. This material can simulate either a complex pattern present within fibro-glandular region of the breast (swirled pattern) or a homogeneous background.
- With cavity (Figure 24)
  The component consists of two halves both having a semi-cavity of a randomly predefined profile. These halves are made of adipose equivalent material, and the cavity is filled with glandular equivalent material. The shape of the cavity can be changed to simulate various structures. The outer shape of the component remains unchanged to ensure interchangeability.

If a bigger volume of the fibro-glandular structure is needed the fibro-glandular region component can be increased in size and take place of one or more "adipose layers".

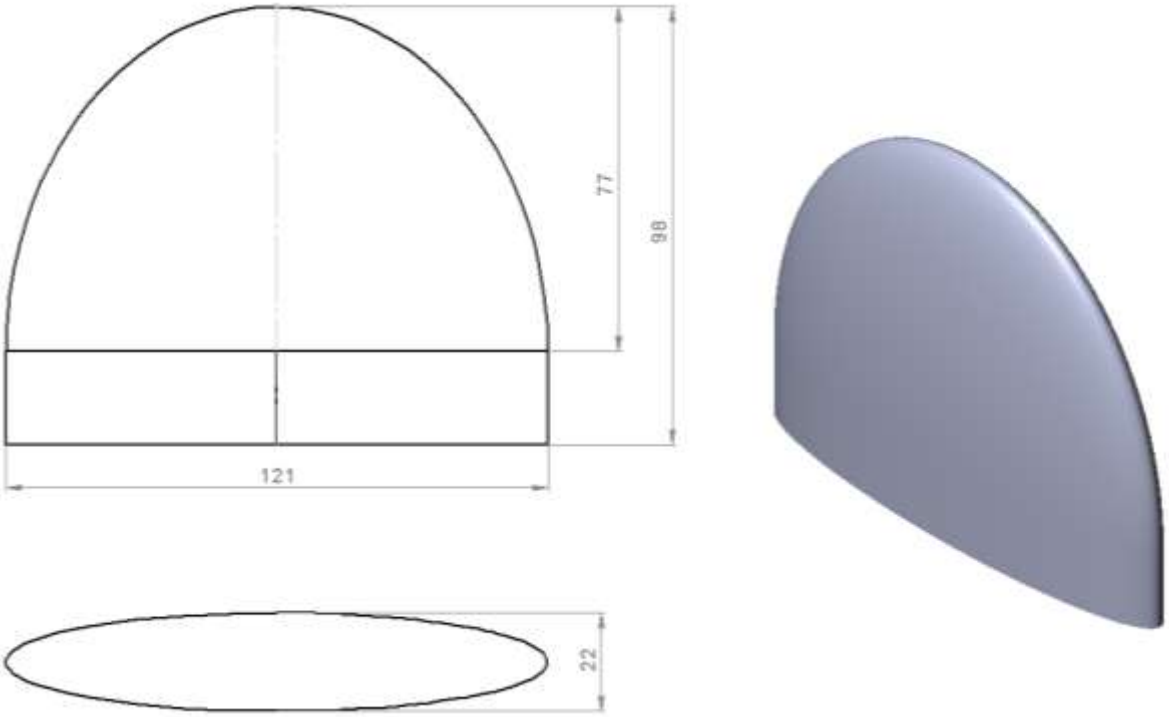

Figure 23: Technical drawing of a single body fibro-glandular region component

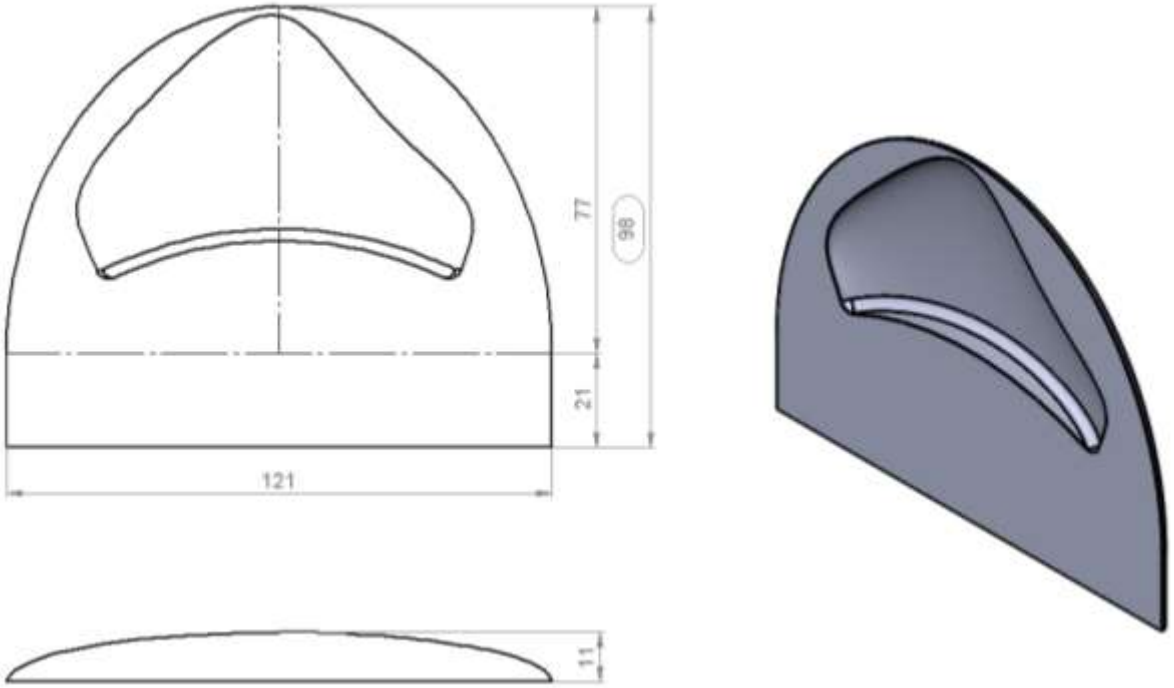

Figure 24: Technical drawing of a fibro-glandular region component with cavity

Chapter 3. Prototyping

Introduction

Prototyping is a crucial part of the designing process, as it allows for an assessment of the design, the identification of mistakes and for performing various tests of the designed object before its mass production.

In this project prototyping phase was used to assess the performance of the modular design of the phantom and to determine implications of using 3D printing technology for manufacturing. For this purpose, components of the phantom were modelled and manufactured using 3D printing technology. Next, the prototype was imaged using a mammography/DBT machine in order to assess how the prototype simulates the breast tissue and consequently adjust the design for real manufacturing.

Methods and Materials

Prototyping process can be divided into ten stages:

1. Development of a prototype model based on the final concept
2. Selection of prototyping technology
3. Selection of materials
4. Adjustment of the model to the used technology and materials
5. Selection of prototyping parameters
6. Manufacturing of the first version of the prototype
7. Imaging of the first prototype
8. Adjustment of the prototype and prototyping parameters
9. Manufacturing of the second prototype
10. Imaging of the second prototype

The model of the phantom presented in the

Final Concept section of Chapter 2 was used to manufacture the prototype.
3D printing was selected as manufacturing technology, because it provides fast manufacturing, and various materials can be used with good fabrication accuracy. Both prototypes were printed using the Leapfrog Creatr Dual extruder; the material selected for fabrication was acrylonitrile butadiene styrene (ABS).
The first prototype (Figure 25) consisted of only three components: two halves of the fibro-glandular region component with a cavity and the 3rd adipose layer, their dimensions were reduced from original dimensions of the final concept by the factor of two. The components were printed with 30% infill[1] of the material and the direction of printing was defined as follows:

1. The FGR components were printed in "lying" position (surface with the biggest area positioned on the working table of the printer) with 45° and 135° inclination of the pattern
2. The 3rd adipose layer (the one "embracing" FGR components) was printed in "standing" position (the dorsal surface of the component lies on the working table of the printer)

The first prototype was imaged using FFDM/DBT machine *Siemens MAMMOMAT Inspiration* (Siemens, Germany).
Next, silicone was poured into the cavities of the core components and the grooves of the adipose layer component; consequent imaging of the obtained prototype was performed to see how the concept works for two different substances.

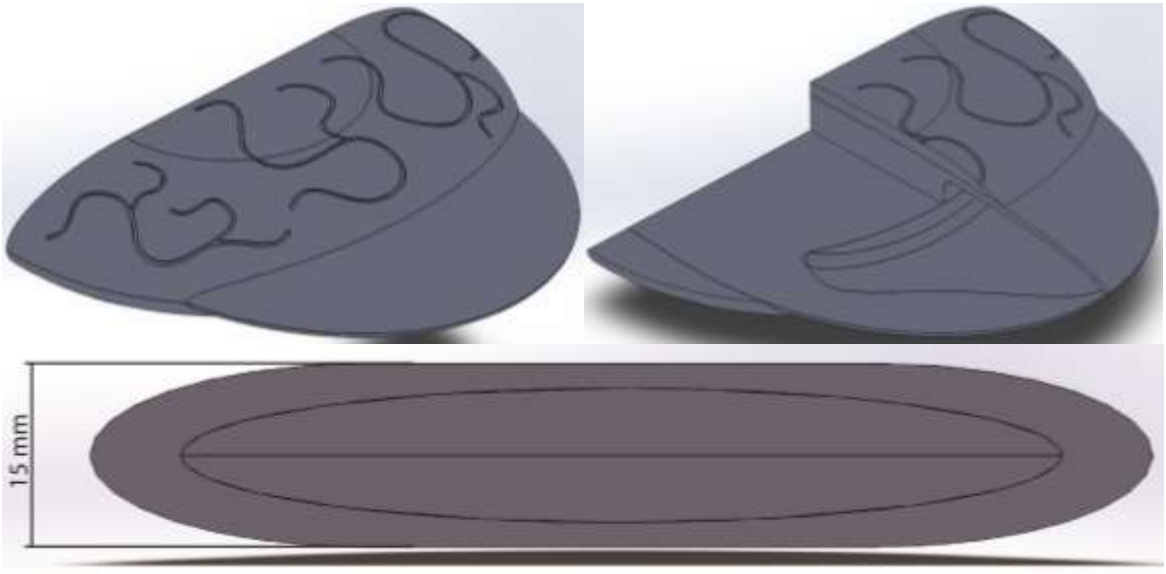

Figure 25: First version of the prototype

After producing the first prototype a modified full-scale prototype was printed (Figure 26), and additional components and objects were manufactured. The final prototype consisted of:

- Two FGR halves components
- Three "adipose" layers
- The 2nd (middle) adipose layer was manufactured in two versions:
    - With grooves on both sides (Figure 27a)
    - One side contained grooves, while the other contained features (Figure 27b):
        - 3 Landoldt rings with different thickness and depth of the profile, and various position of the gap

[1] Infill parameter determines the percentage of bulk volume occupied by 3D printing material. It can also be defined as a parameter inverse to porosity, e.g. 30% infill equals 70% porosity.

- 5 lines of various thickness, depth and gap between each pair of lines

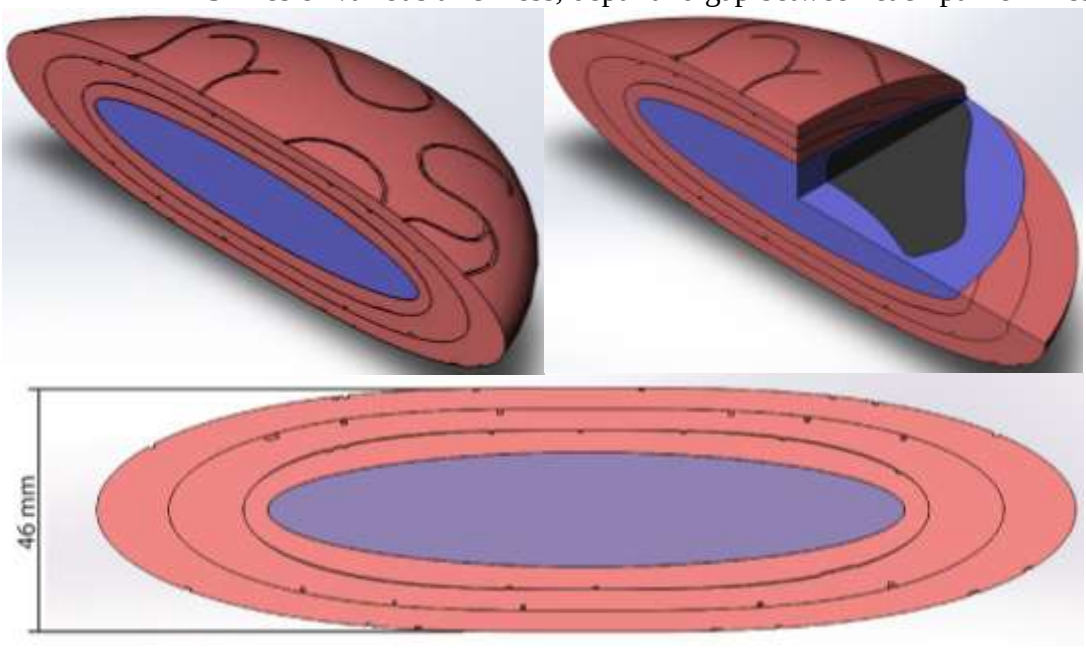

Figure 26: Second version of the prototype

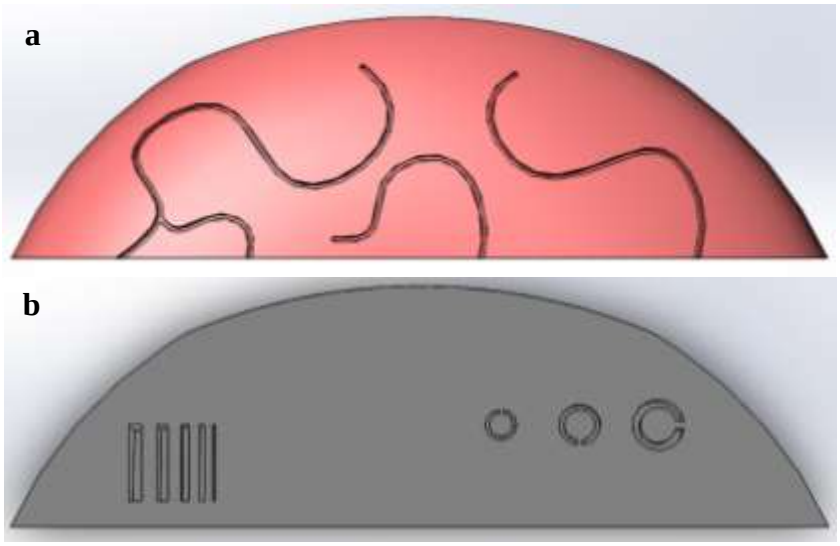

Figure 27: Two versions of the middle layer: *a* – with grooves mimicking glandular structures; *b* – with features for initial image quality assessment

The model was modified for prototyping by removing the flat region of the model to reduce the time and material necessary for 3D printing. This change did not affect the results in any way, as most structures of interest are located within the preserved part of the model (e.g. fibro-glandular region, grooves mimicking the glandular structures). All components were printed in the standing position to avoid the formation of the pattern in transverse plane and the value of the infill parameter was set to 25%. Next, the cavities and the grooves were filled with silicone. An additional object, a 1 cm^3 3D printed resin cube, was introduced into the silicone-filled cavity of the fibro-glandular region component to assess DBT and FFDM modalities in detection of foreign object within an environment with homogeneous X-ray attenuation.

For printing a grid pattern was selected to reduce its appearance on consequent X-ray scans (Figure 28) [**Ошибка! Источник ссылки не найден.**]. Different values of the infill parameter result in different attenuation of incident radiation, e.g. lowering infill value lowers attenuation and vice versa.

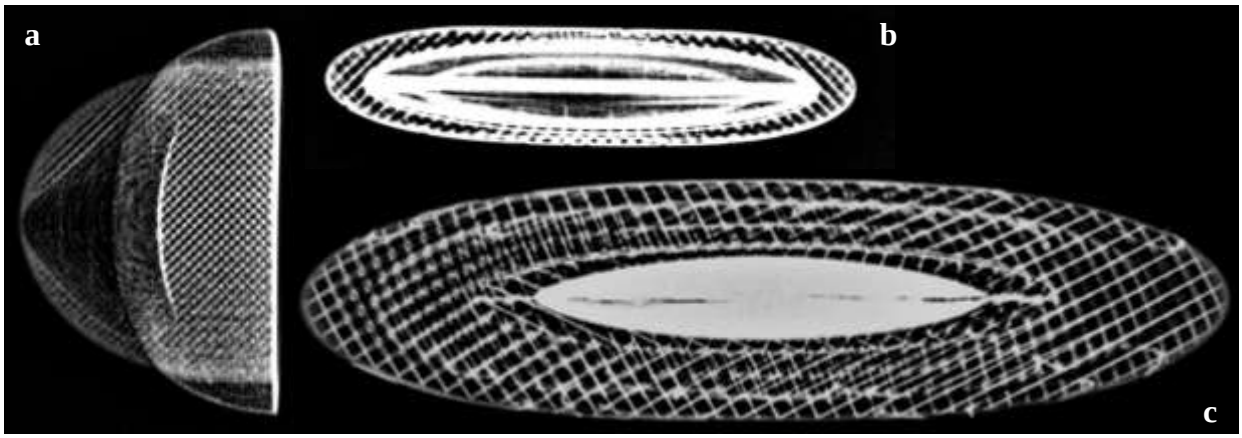

Figure 28: 3D printing pattern: *a, b* – first prototype; *c* – second

After fabrication both prototypes were imaged using FFDM/DBT machine Siemens MAMMOMAT Inspiration at following voltages:

- FFDM – 25.6 kV
- DBT – 5 kV per image

The obtained DICOM images were extracted from the server and inspected using RadiAnt DICOM Viewer.

Results and Discussion

First prototype

Images obtained by imaging of the first prototype in assembled state are presented in Figure 29.

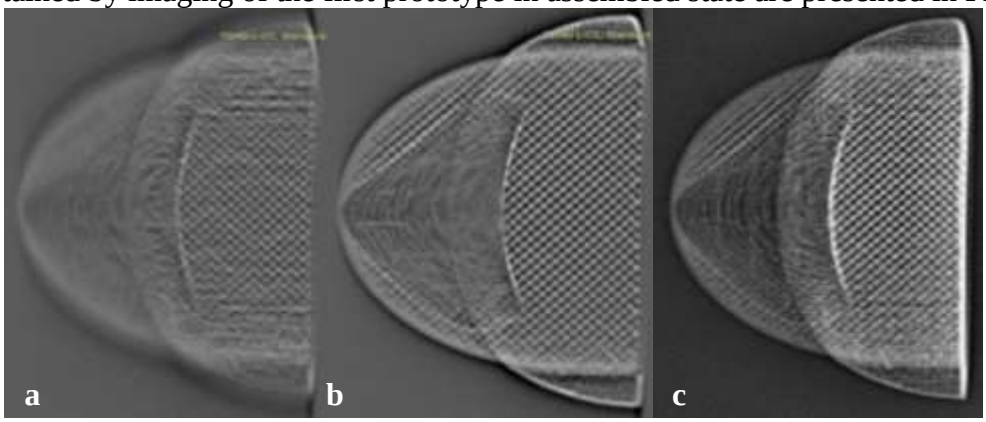

Figure 29: Imaging of the first prototype: *a* – top DBT slice; *b* – median DBT slice; *c* – FFDM image

Superimposition of differently directed 3D printing patterns of the core components and the 3rd adipose layer of the first prototype completely obscures the empty grooves in the FFDM image (Figure 29c), whereas the top DBT slice (Figure 30a) shows a barely seen profile of the grooves. However, in the latter case it is still seen only when the observer is aware of the grooves profile.
Without adjusting the image window FFDM provides a less noisy image of the phantom which is defined by lower dose used for each single scan and additional reconstruction in DBT modality.
The obtained images show a strong pattern present in two middle (FGR) components due to the "lying" position of printing, however, the "standing" printing position of the adipose layer showed hardly any distinguishable pattern.
Additional imaging of the adipose layer component was performed in order to assess sensitivity of FFDM and DBT modalities in detection of shallow grooves on the surface of the component (Figure 30).

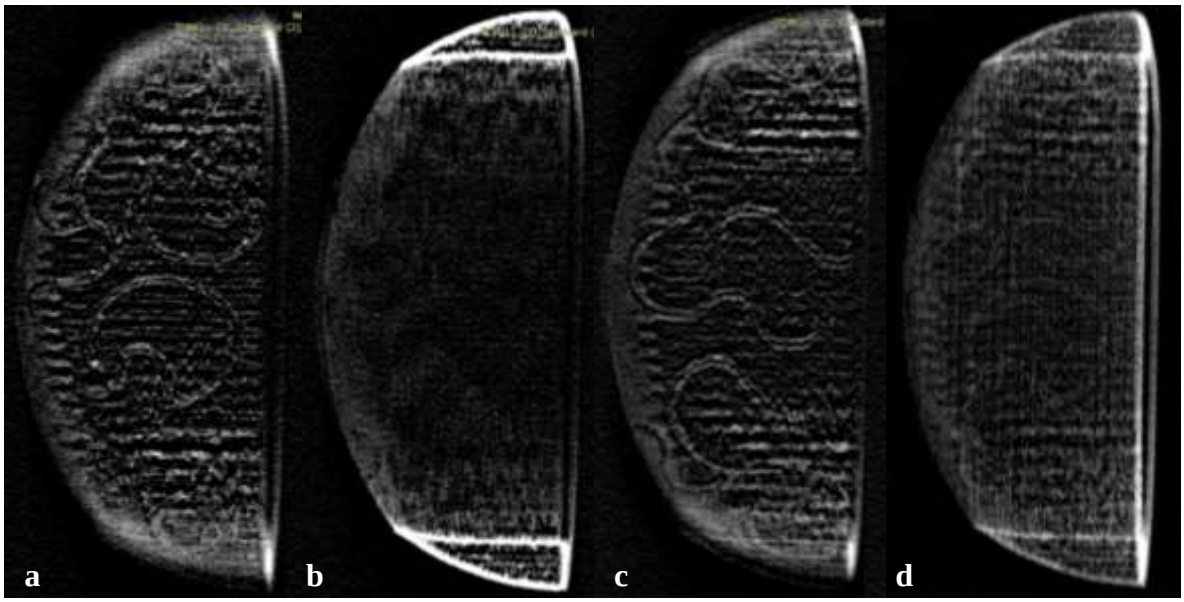

Figure 30: a - bottom DBT slice (z=0 mm); b - median DBT slice (z=7 mm); c – top DBT slice (z=15 mm); d – FFDM image

Figure 30 shows a difference between DBT and FFDM: DBT is able to reconstruct the thin walls of the grooves on the surface of the core component, while in the FFDM image these walls are visible only when an observer knows about their presence.

The results of imaging the first prototype after filling the grooves with silicone can be seen in Figure 31 and Figure 32.

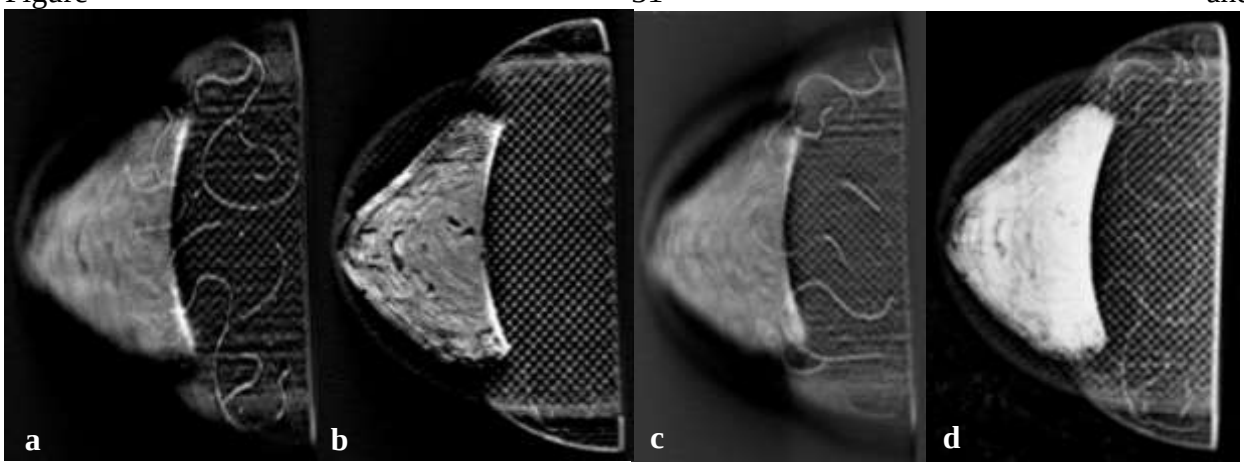

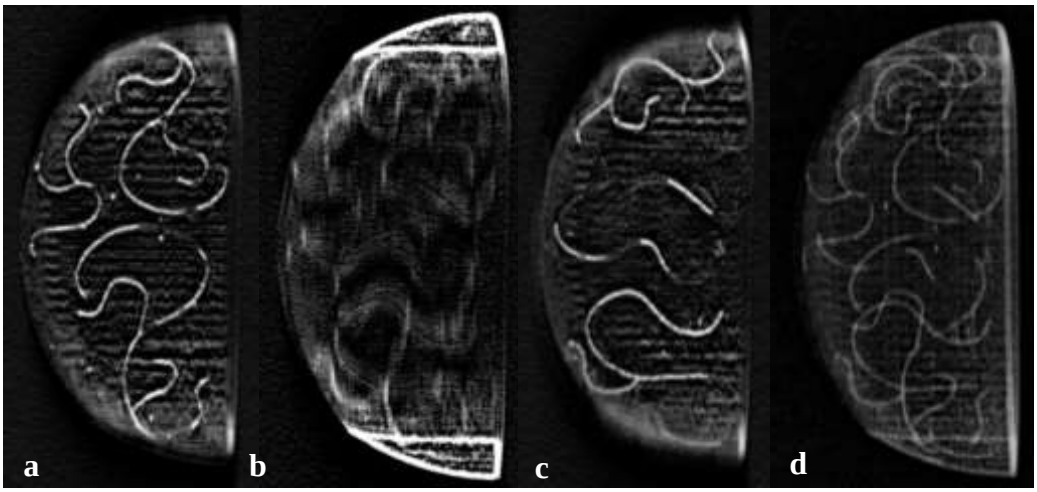

Figure 31: Adipose layer of the first prototype: *a* – top DBT slice; *b* – median DBT slice; *c* – bottom DBT slice; *d* – FFDM image

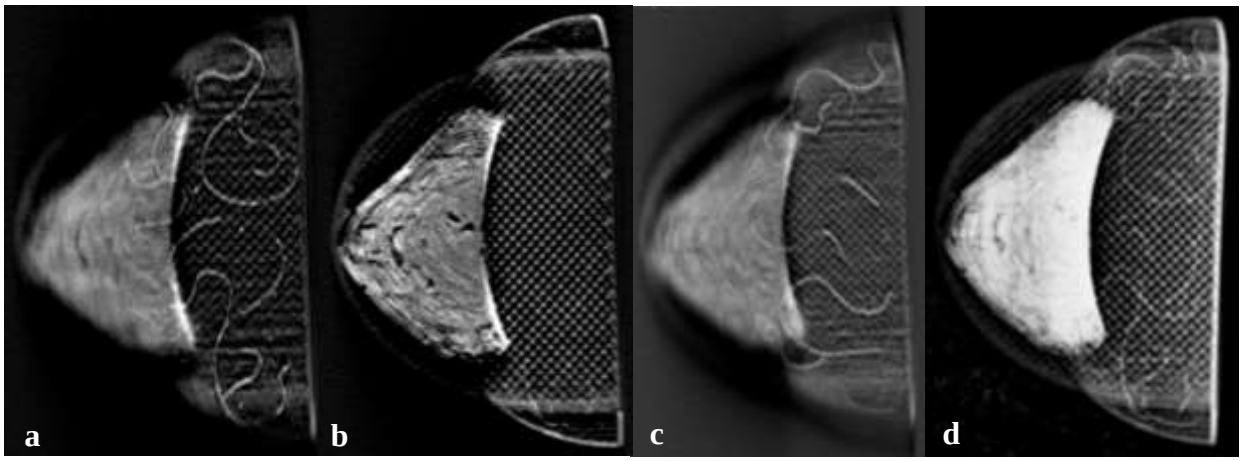

Figure 32: Silicone filled first prototype in assembled state: *a* – top DBT slice; *b* – median DBT slice; *c* – bottom DBT slice; *d* – FFDM image

As can be seen in Figure 30 andFigure 31 median DBT slices of the adipose layer show strong attenuation by walls; FFDM image does not have similar strong contrast.

Second prototype

Figure 33 presents mammographic scan of all components of the final prototype:

- 2 FGR components (halves forming single body of the FGR component) with a cavity
- 1st adipose layer (outer)
- 2nd adipose layer (middle) in two versions:
  - Grooves on both sides
  - 3 Landoldt rings and 5 resolution lines on one surface, grooves on the other
- 3rd layer (inner)

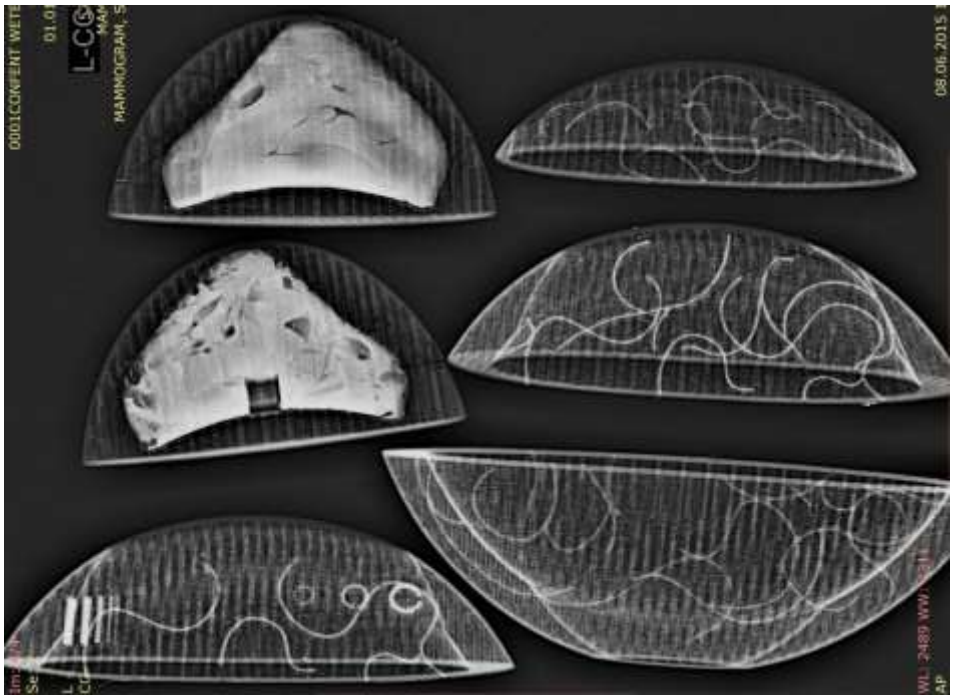

Figure 33: FFDM Image of all components of the final prototype in dissassembled state

First, imaging of assembled prototype with the adipose layer containing features was performed; the obtained images are presented in Figure 34.

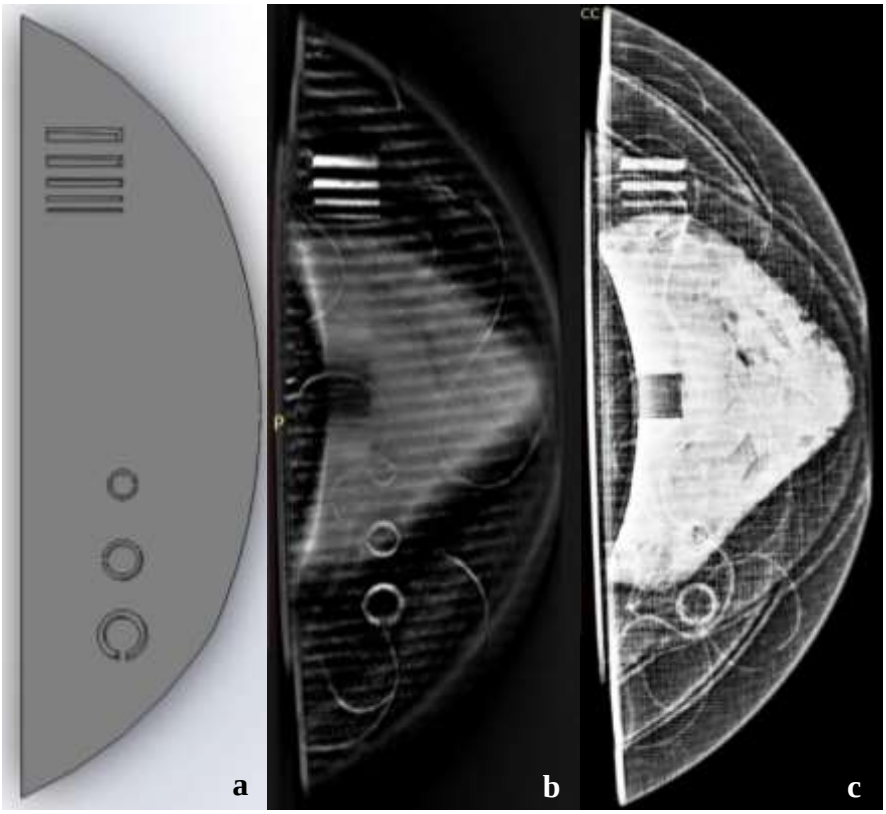

Figure 34: Assembled second prototype with feature containing layer: *a* – 3D CAD model; *b* – DBT image; *c* – FFDM image

Figure 34 clearly shows that DBT present clearer image of the features, both Landoldt rings and resolution lines. However, on both images the last (bottom) resolution line, which can be seen on the model, is obscured by different structures: by appearing 3D printing pattern in the DBT

image, and by silicone within the FGR component in the FFDM image. Detailed images of the Landoldt rings are presented by Figure 35.

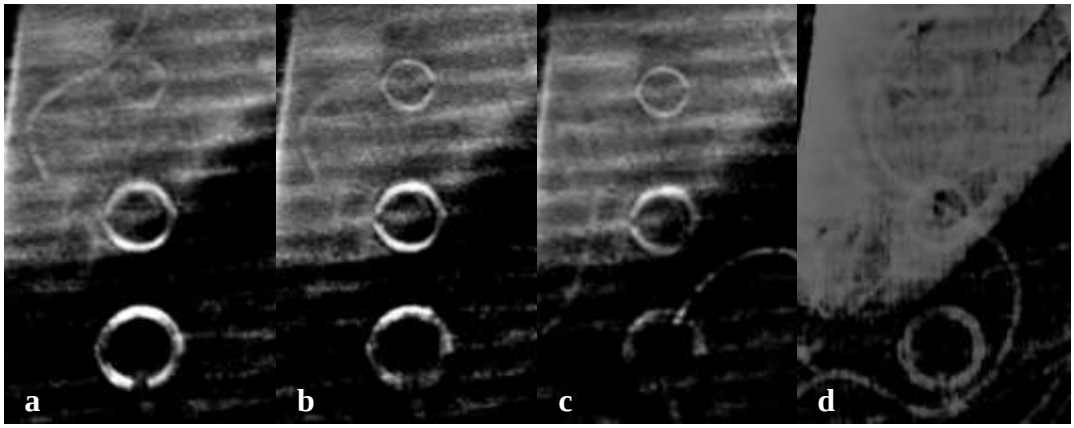

Figure 35: Detailed view of the Landoldt rings: *a* – DBT slice (z = 35 mm); *b* – DBT slice (z = 36 mm); *c* – DBT slice (z = 37 mm); *d* – adjusted FFDM image

The smallest ring appears also in the FFDM image after adjusting image window (Figure 35c); however no clear gap can be seen in it, at the same time slice-specific DBT images provide clear image of gaps within each ring.

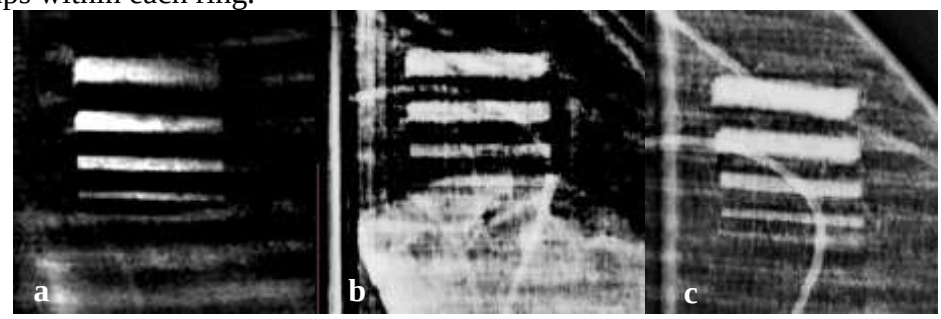

Figure 36: Detailed view of the resolution lines: *a* – DBT image; *b* – FFDM image; *c* – FFDM image of the separate feature layer

Figure 36 provides detailed images of the resolution lines for both DBT and FFDM, additional image of the separate feature containing component clearly indicates the presence of the bottom line.

The smallest Landoldt ring can be seen in the images of both modalities (Figure 36), however, only in DBT image a small gap in each ring can be distinguished. Resolution lines are also better seen on the DBT image. Although not seen due to the presence of 3D printing pattern the most right resolution line could also be seen on the DBT image, while the superposition of structures present on FFDM image results in complete obscuring of the line.

Both DBT and FFDM scans show high attenuation by walls of the 3D printed components, this occurs due to 100% infill at the wall surface of the components (Figure 37). Setting the printer to retain porous pattern at the wall surface still results in high attenuation of the wall. This is most likely to occur because of characteristics of the 3D printer and thermosetting properties of the material [**Ошибка! Источник ссылки не найден.**].

Additionally, misalignment of the components can be seen; it is justified by deformation of 3D printing material. Therefore additional adjustment of tolerances is required for proper alignment of the components should 3D printing be chosen as manufacturing technology.

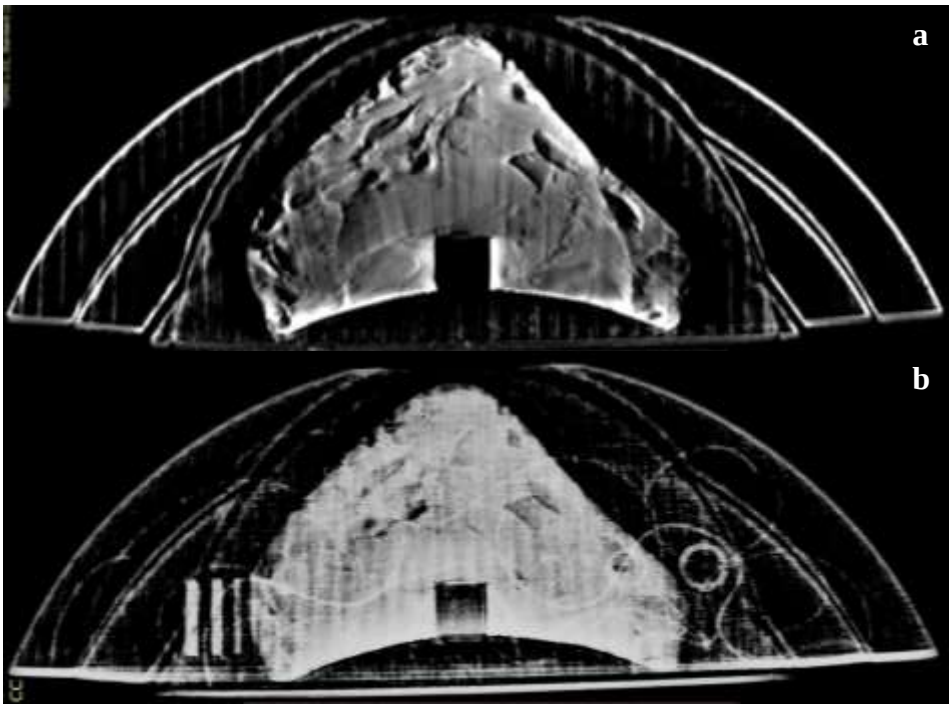

Figure 37: Appearance of the 3D pattern and wall attenuation: *a* – DBT image; *b* – FFDM image

Conclusion: Prototyping

Manufacturing and imaging of the prototype phantom provided information on various characteristics of phantom design, phantom fabrication, and modality performance.

DBT appears to allow for better identification of very thin interfaces, such as the walls of the empty grooves on the surface of the first phantom prototype. DBT also provides better appreciation of the imaged objects, which are otherwise partially or completely obscured by over- or underlying structures in FFDM images. Slice-specific representation enables more options for appreciating small features unseen on FFDM image, e.g. the gaps in Landoldt rings or the thin lines.

Infill pattern allows for an implementation of objects with different radiodensities using a single material. However, even slight presence of the 3D printing pattern artifact in the images decreases overall image quality and obscures objects and structures identification.

The idea of using modular design of the phantom proves to be plausible, as variation of components of the phantom provides more options for evaluation of breast imaging modalities, in this case DBT and FFDM. However, during the production of the phantom additional testing of 3D printing materials and technologies is necessary to ensure the quality of fabrication using 3D printing. Another drawback of 3D printing or at least of the chosen prototyping technology is its higher radiodensity of the wall region of the components; therefore, other 3D printing techniques should be investigated to alleviate this problem.

Chapter 4. Manufacturing

Introduction

To ensure the success of the experimental concept of the phantom it is good to present several techniques for its production. Therefore in this section three technologies for phantom manufacturing are discussed:

- Casting using epoxy based resins
- 3D printing
- 3D printing combined with casting

For each of these techniques materials, necessary equipment, and specific production characteristics are presented.
Structure of the chapter is component-specific and provides information on manufacturing technologies and materials necessary for fabrication of phantom components.

Skin layer

For all variants of manufacturing the skin layer, which also plays a role of a protective shell of the phantom, is made of PMMA. At the thickness of 2 mm, PMMA has the attenuation similar to real skin [21]. The skin layer can be produced by machining a PMMA block or casting it into the desired shape.

Adipose layers and fibro-glandular region

This section reviews manufacturing of components mimicking internal breast structures and adipose compartments. Fabrication materials and methods are discussed for each manufacturing technique.

Epoxy Resin Casting

Casting of epoxy based resins is one of currently used techniques for production of breast phantoms, e.g. commercial phantom CIRS BR3D is manufactured by casting epoxy resins with X-ray parameters equivalent to real breast tissues [13]. However, usually casted in slabs, epoxy resins can also be casted in the shape of the components of the here designed concept as their shape is defined only by the shape of a mould the resins are casted in.
The general procedure of epoxy resin casting is presented in Figure 38.

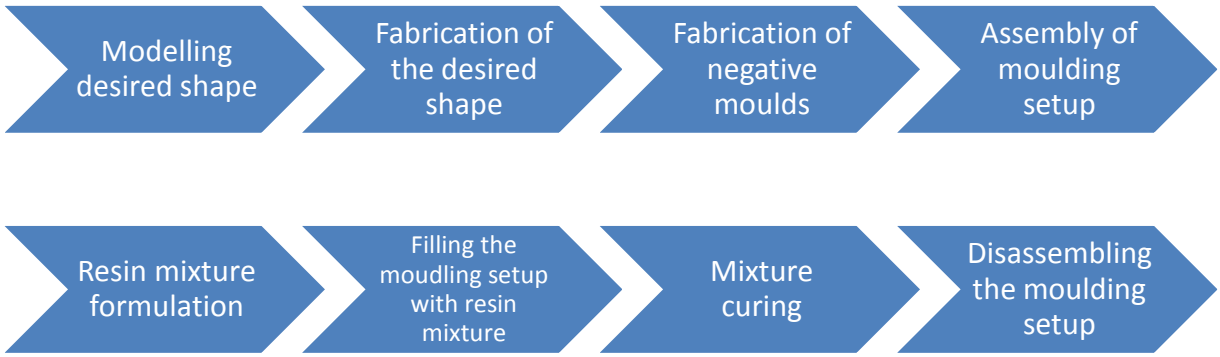

Figure 38: General procedure of epoxy resin casting

First, a model of a desired shape and a cavity component must be made in CAD software (for example, SolidWorks), which will be used as a positive mould. Next, the desired model and the cavity component are manufactured either by machining or 3D printing.

To make a negative mould, the desired shape is placed into the cavity component and the resulting casting pattern is filled with silicone rubber (Figure 39).

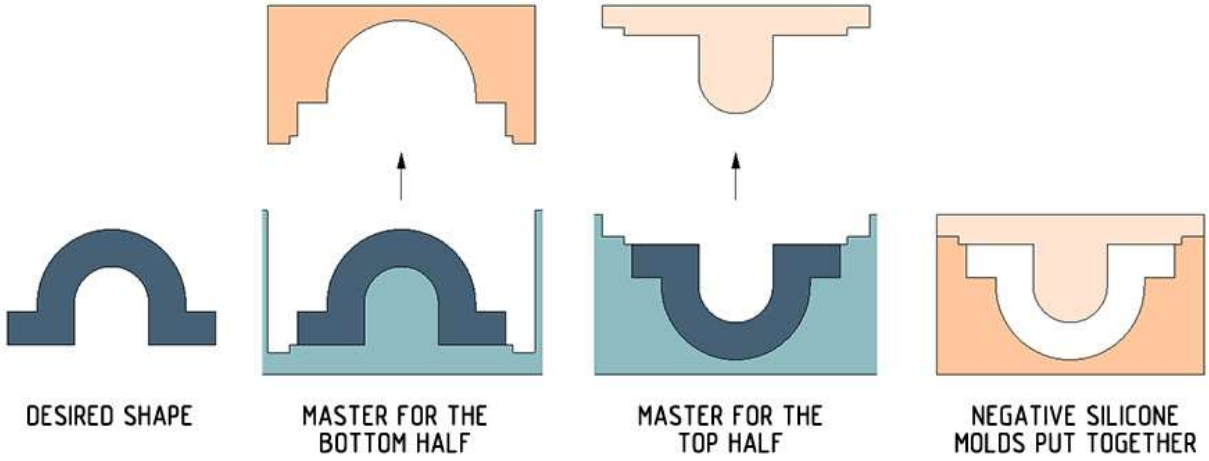

Figure 39: Procedure of preparation of silicone mould setup [22]

Figure 40 shows the aforementioned process applied to the designed phantom additionally presenting possible mould design for the first adipose layer.

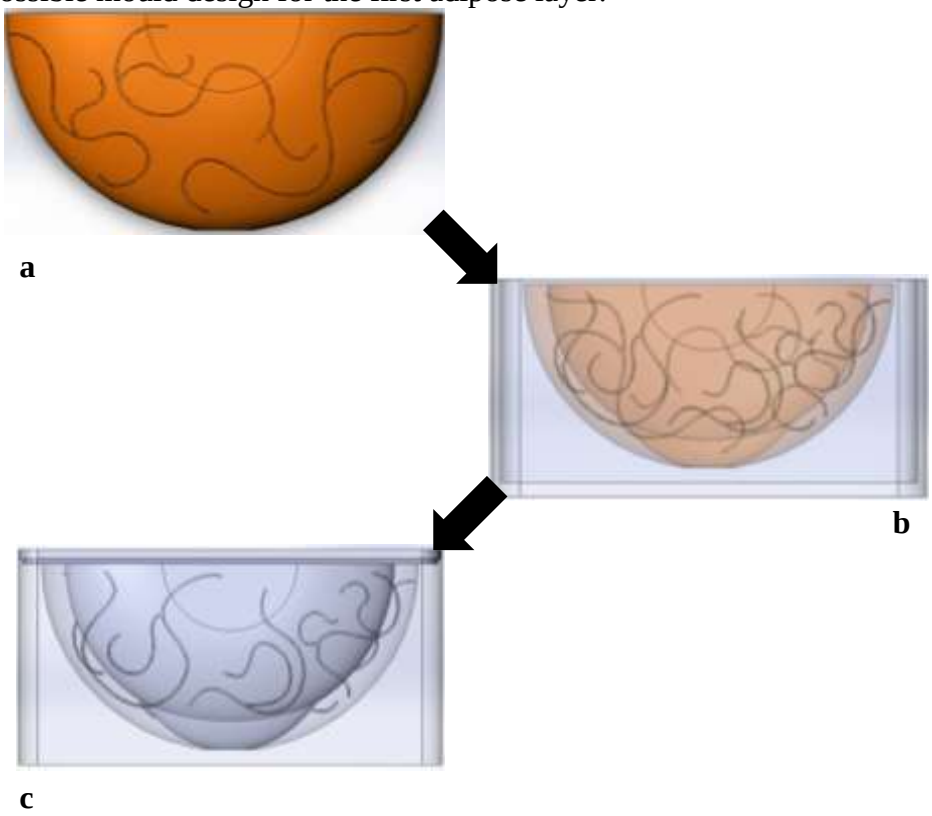

Figure 40: Manufacturing of the mould setup: *a* – an adipose layer manufactured by 3D printing (or conventional machining); *b* – bottom silicone master; *c* – complete moulding setup (adipose layer shape is removed)

Various silicones can be used but the two-component platinum-catalyzed silicones have optimal characteristics for this purpose [22]; these silicones have no polymerization byproducts, exhibit no shrinkage, have excellent mechanical properties, can be stored indefinitely, and provide easy detachment of the mould from the casted body. An additional advantage of moulds made of platinum-catalyzed silicones is their high overall accuracy (up to 5 μm) [22]. To remove air bubbles present in the silicone mould, a special degassing jar can be used, where, by applying vacuum, the mould will obtain a better surface resulting in high accuracy of casting.

Different components of the phantom will have different X-ray density in terms of fractions of adipose and glandular equivalency. Epoxy based resin used for the production of tissue equivalent phantom components will have varying composition by weight fractions [23]. Components and their quantities required for making the resins are presented in Table 6.

Table 6: Tissue-equivalent material composition by weight percent for 100% glandular and 100% adipose tissues [23]

Substance	100% glandular	100% adipose
Araldite GY 60-10 (epoxy resin)	49.43%	48.43%
Jeffamine T-403 (hardener)	19.77%	19.37%
Polyethylene powder (medium density)	18.5%	26.3%
Phenolic microspeheres	0.88%	1.2%
Magnesum oxide powder	11.42%	4.7%

Variation of the resin composition enables creation of different structures mimicking real breast structures.

To fabricate the resin the following procedure must be performed:

1. Prepare and weigh the necessary quantities of substances for certain values of glandularity:
    - Araldite GY 60-10 (epoxy resin)
    - Polyethylene powder (medium density)
    - Magnesium oxide powder
    - Phenolic microspheres
    - Jeffamine T-403 (hardener)
2. Add the substances in the order mentioned above and thoroughly mix them
3. After adding the hardener mix the mixture for at least 20 minutes to remove air bubbles (vacuum degassing is beneficial for air removal)

The following steps are to be taken to cast a phantom component using the prepared resin:

4. 3D print or use Computer Numerical Control (CNC) machining to fabricate a desired shape
5. Cast silicone mould components
6. Assemble the mould
7. Apply a mould release agent (spray is preferred; no waxes can be used, otherwise it will result in damaged casted part)
8. Pour the mixture into the moulds and let it cure for 48 hours (for 1 cm thickness of the resin part; for other thicknesses time may vary)
9. Disassemble the mould and release the casted component

Simplest way to produce an adipose component of the phantom on the basis of the final concept is done by:

1. Preparing adipose equivalent mixture
2. Casting the adipose part of the adipose layer component with grooves
3. Preparing glandular equivalent mixture
4. Filling in the grooves
5. Polishing the excessive glandular equivalent resin until the initial shape of the adipose part is reached (CNC machining might prove beneficial to ensure high accuracy)

This manufacturing approach enables fabrication of the phantom in laboratory setup; if the moulds are not prepared using 3D printing but machining a proper workshop is needed, for example presence of CNC machine is beneficial for accuracy. Highly accurate moulds provide good compatibility of different components ensuring modular structure of the phantom. Modern production techniques allow for the fabrication of complex shapes ensuring the possibility of casting a phantom with very complex structure.

3D printing

3D printing is one of the most recent manufacturing technologies; it is extensively used for rapid prototyping. Current 3D printers can work with different materials (e.g. plastics, metals, ceramics, etc.) fabricating multi material bodies.

Penn phantom is a significant example of applying 3D printing for fabrication of complex breast phantoms [15]. However, in that case only glandular structures of the phantom were printed, while the adipose compartments were casted using epoxy based resins. Contrary to the Penn phantom where slabs were printed for the project an option to print complete phantom components is investigated.

Unlike the article of Penn et al. which was published in 2012, recent developments in 3D printing technology might have a solution for printing both glandular structures and adipose compartments using epoxy based resins. The study of Compton and Lewis presents technology of printing epoxy resin inks using thermosetting 3D printer [24].

During the prototyping phase it was discovered that although mechanical, chemical and other properties of 3D printing materials are known, it would be necessary to perform preliminary testing of the 3D printing materials: quantify excessive shrinkage, expansion or deformation of the materials during their thermosetting in the course of the 3D printing process. Information about these parameters would ensure the accuracy of 3D printed components

3D printing and casting

This technique would combine 3D printing and casting procedures. Printer would be used for manufacturing the glandular structures and epoxy resin for adipose tissue.

Adipose layers

Similar to the Penn phantom glandular structures can be 3D printed with the material FC720 (Objet Geometries Inc., Rehovot, Israel) using a polyjet 3D printer [15]. The structures could be designed in the way to ensure connection of all cavities which later would be filled with epoxy resin mimicking adipose tissue. The printed structure is placed into the silicone mould, which is later filled with the epoxy resin (Figure 41).

Fibro-glandular region

Complex glandular structure of the core region can also be 3D printed. The structure is then placed into the casting mould, and special positioning features added to the structure will ensure proper placement of the structure within the mould. Next, the mould is filled with epoxy resin with X-ray parameters equivalent of the adipose tissue (Figure 41).

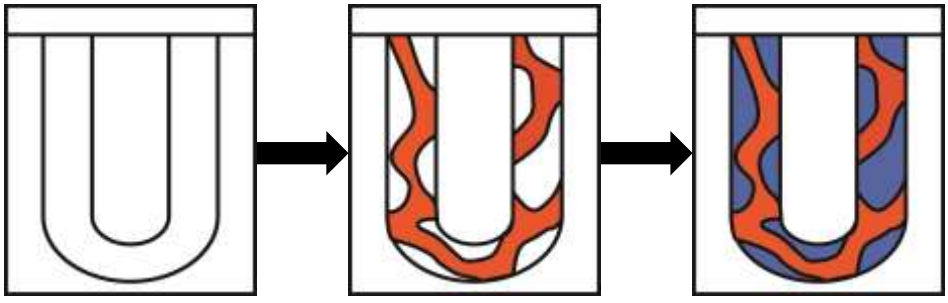

Figure 41: Combination of casting and 3D printing: Silicone mould setup is prepared, next, 3D printed glandular structure is places into the mould, which is later filled with epoxy resin mixture

Selection of manufacturing technique

Of the three presented techniques only casting is currently implementable in laboratory setup, as complete 3D printing using epoxy resins is still to be developed and there is no evidence of 3D printer capable to print a multi material phantom with other tissue equivalent materials. Combining 3D printing might prove justified, however the resulting price will be higher than for

complete casting due to use of Polyjet 3D printer. ***Therefore, the casting approach is chosen as the main manufactruing technique.***

Review of alternative materials

In order to ensure further development of the phantom the last section of this chapter discusses a number of materials applicable to phantom manufacturing. The discussed materials are reviewed regarding their attenuating and scattering properties when mimicking breast tissues.

- Poly(methyl methacrylate) (PMMA) – Glandular tissue
  Scattering signature of PMMA is also different from that of adipose tissue and it has a big discrepancy with scattering profile of glandular tissue (Figure 43) [25]. Attenuating properties of PMMA are close to that of 50/50 composition of the breast (Figure 42); however PMMA cannot be used as a substitute to neither 100% adipose or 100% glandular tissue [26]. Therefore, PMMA cannot be used as an adequate material for simulation of glandular tissue.

- Water – Glandular/muscle tissue
  Both studies of Poletti et al. [25] and Geraldelli et al. [28] support the idea of mimicking glandular tissue with water by showing scattering signature of water similar to the signature of glandular/muscle tissue (Figure 43 and Figure 44). Study of Geraldelli also shows similar attenuation profile of water and muscle tissue. Therefore, water can be seen as a perfect equivalent to glandular/muscle tissue.

- BR12 (CIRS/RMI) – Adipose tissue
  According to study of [21] BR12-CIRS epoxy based resin is a mediocre substitute to adipose tissue, as at low energy levels it has attenuation similar to adipose tissue, while for higher energy it shifts to 50/50 breast composition. Investigation of scattering signatures of both BR12-CIRS and BR12-RMI performed by Poletti et al. [25] shows close similarity of these materials to the signature of adipose tissue.

- 062A-11 (CIRS) – Adipose tissue
  Study of Geraldelli [28] shows that 062A-11 material by CIRS company (denoted as *adipose-equivalent material* in [28]) has attenuation close to theoretical values of attenuation of adipose tissue along the whole presented energy range. Scattering signature of this material occurs to be similar to the adipose tissue, thus making this material a good candidate for adipose tissue substitute in a phantom.

- Polyethylene (PET) – Adipose tissue
  When normalized to water adipose tissue and polyethylene have close attenuation profile along a range of energies [21], however without normalization a certain difference can be seen between two substances, in the low energy region particularly [26]. Scattering signature also differs resulting in imperfect simulation of adipose tissue by PET [27].

- Calcium carbonate – Microcalcifications
  Calcium carbonate ($CaCO_3$) is widely used for simulation of microcalcifications in breast phantoms [29,30], as it has similar attenuation to that of natural calcifications.

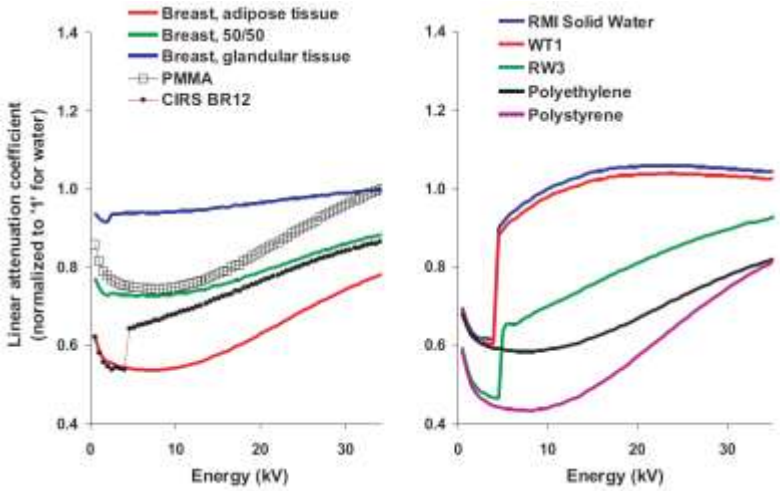

Figure 42: Linear attenuation of materials investigated in the study of Skrzyński et al. [21]

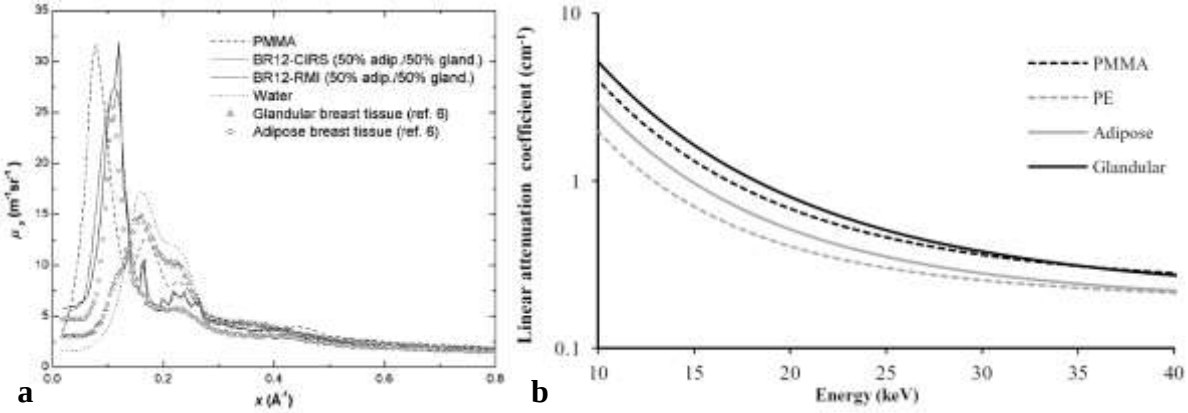

Figure 43: Scatterin signatues and linear attenuation of some materials compared to breast tissues: *a* – scattering signatures of materials investigated in the study of Poletti et al. [25]; *b* – linear attenuation of PMMA and PET compared to breast tissues in the study of Bouwman et al. [26]

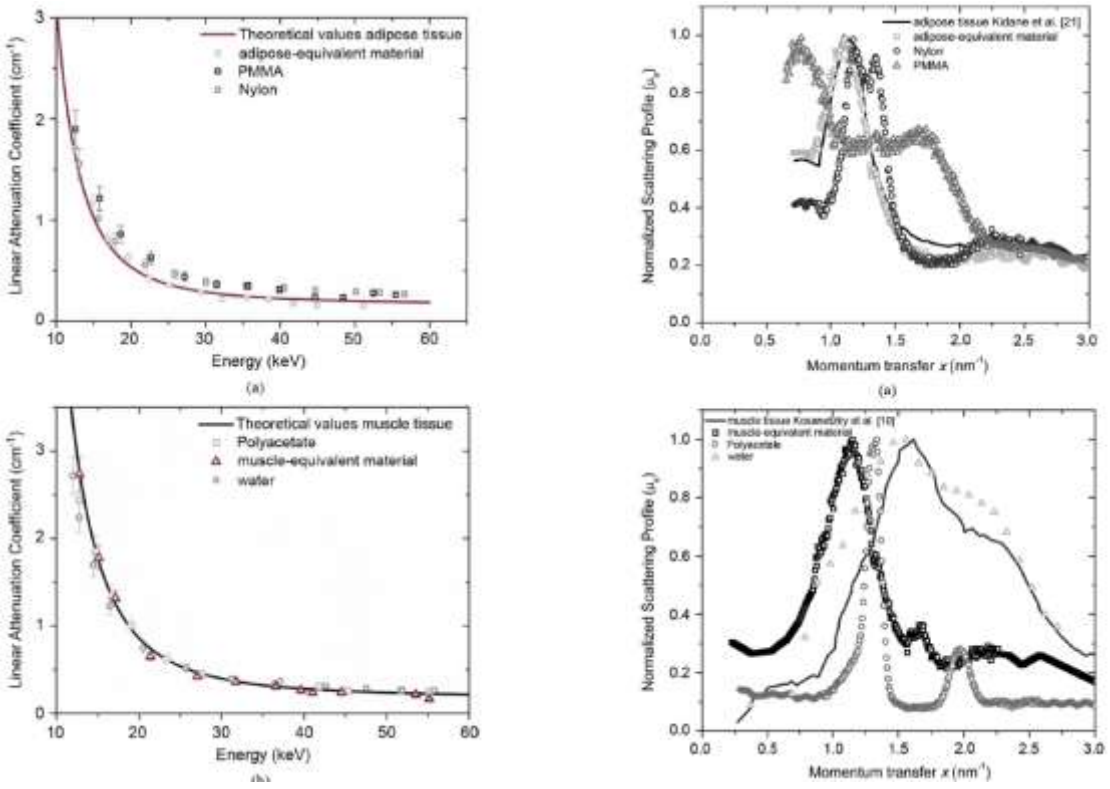

Figure 44: Linear attenuation and scattering signatures of phantom materials and breast tissues [28]

Moulds for epoxy resin casting

Selection of the epoxy resin casting technique as the main manufacturing approach requires further investigation of the process. Therefore, this section presents 3D models of the moulds which can be used for manufacturing of adipose layers and FGR components of the phantom.
Figure 45 shows how the bottom negative master can be assembled using four segments to provide proper glandular pattern without damaging at the stage of mould disassembling and release of the casted part.

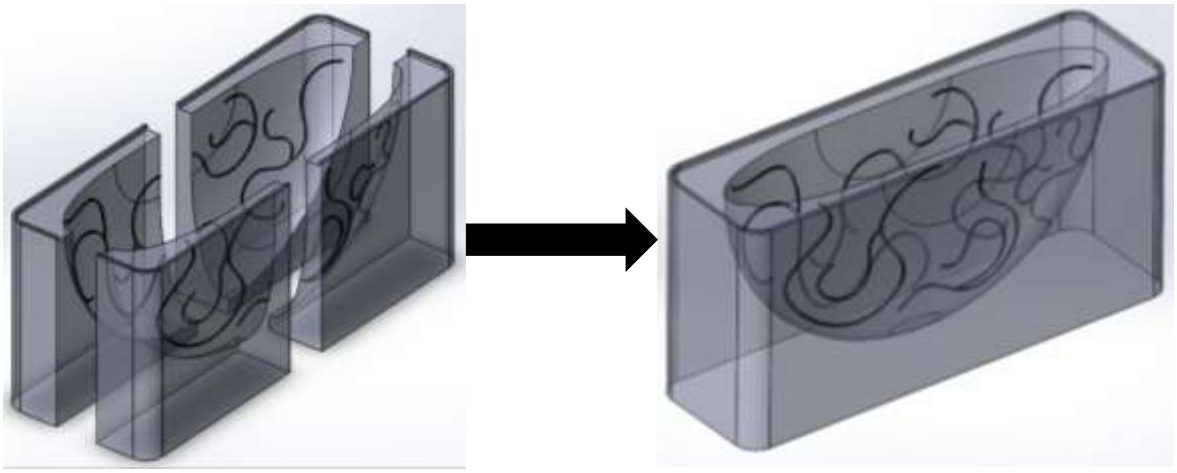

Figure 45: Assembling of the bottom master

Figure 46 presents complete moulding setup: first the bottom master is assembled, next a top negative master is added completeing the mould setup.

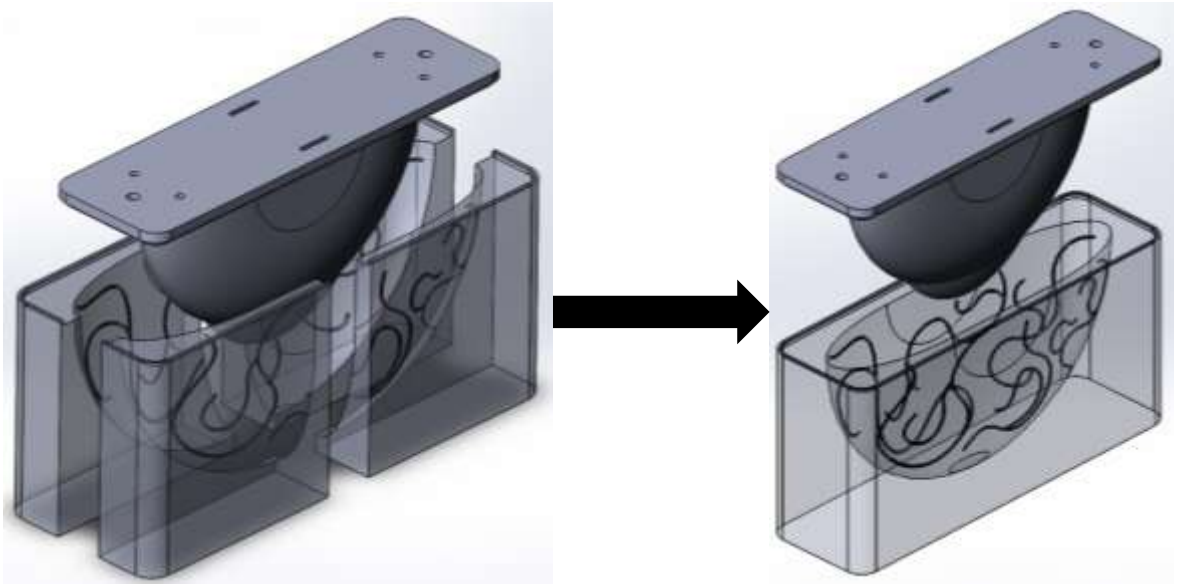

Figure 46: Complete mould setup

3D models of mould setups for casting of adipose layers and fibro-glandular region components are shown in the Figure 47. For casting of the phantom a two-body version is selected to provide higher further variability of mimicking breast structure.
Figure 48 is a representation of how epoxy resin mixture can be injected into a mould to cast a phantom component. The resin is introduced via a set of inlets, once the mould is completely filled excessive mixture will pour out of inlets marking the beginning of curing phase.

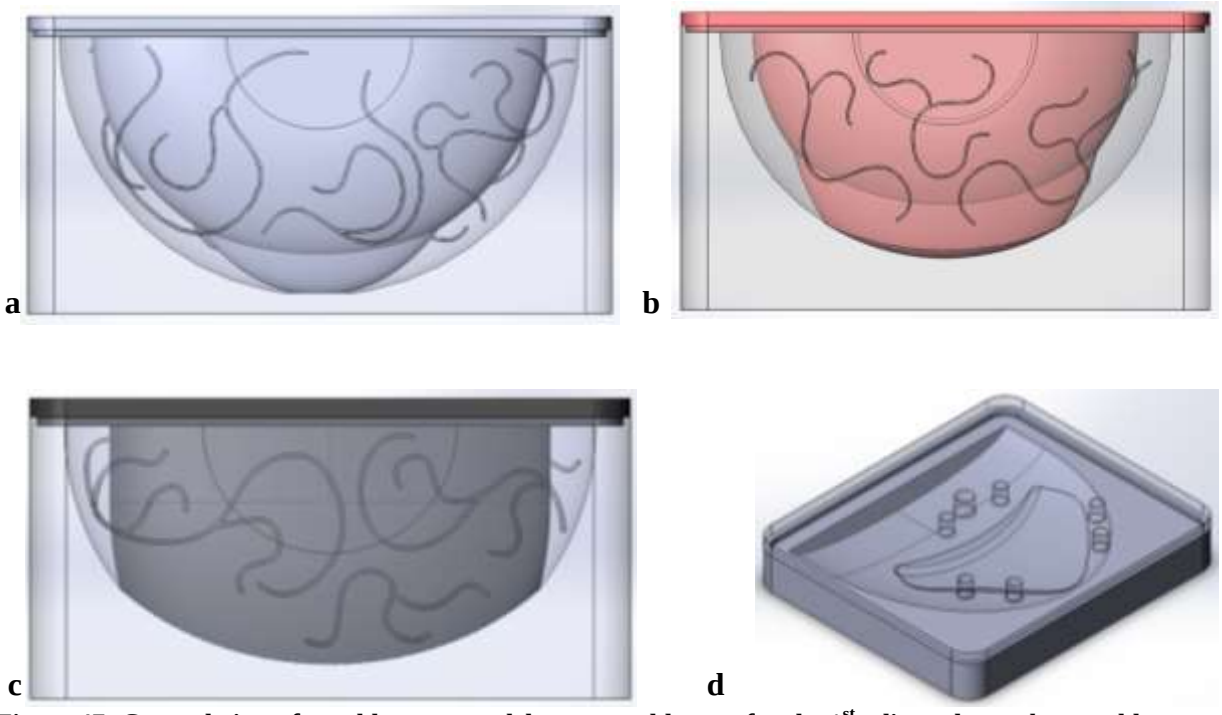

Figure 47: General view of mould setups models: *a* – mould setup for the 1st adipose layer; *b* – mould setup for the 2nd adipose layer; *c* – mould setup for the 3rd adipose layer; *d* – mould setup for the half of fivbroglandular-component with cavity

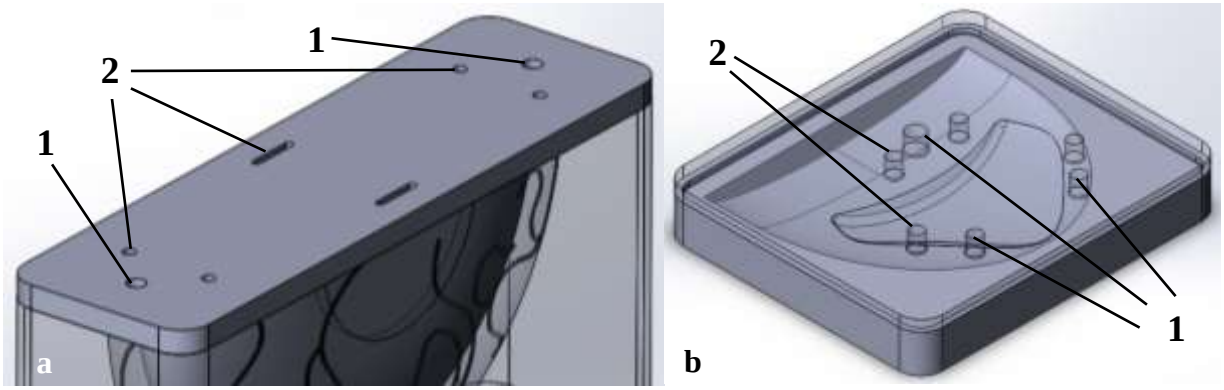

Figure 48: Top master of a mould setup: *a* – for adipose layer components; *b* – for fibro-glandular components; 1 – inlets to feed in the epoxy resin mixture, 2 – outlets to let excessive epoxy resin mixture flow out (marking complete filling of the mould)

Stress analysis of manufactured phantom

During exploitation stage the phantom will be subjected to different mechanical effects, and the main among them is compression by a paddle of a mammography/DBT machine. This section presents results of finite element analysis modelling of phantom components which are subjected to compression.

According to the list of requirements a compression force of 150 N was selected as a reference. Compression was modeled for each separate component. The compression force was applied to the top plane of the component, while the bottom plane was designated as a fixture to simulate placement of the phantom on the table of the imaging machine.

Table 7 contains mechanical properties of PMMA material used for fabrication of the skin layer component.

Table 7: Mechanical properties of PMMA

Parameter	Value
Density	1150-1190 kg/m^3
Young's modulus	2.2 – 3.8 GPa
Ultimate strength (tensile)	47-79 MPa
Poisson's ratio	0.35

Figure 49 shows compression of the skin layer component, maximum stresses within the component are lower than minimum ultimate strength at least by a factor of 10. Thus, the component will withstand the prescribed load of 150 N.

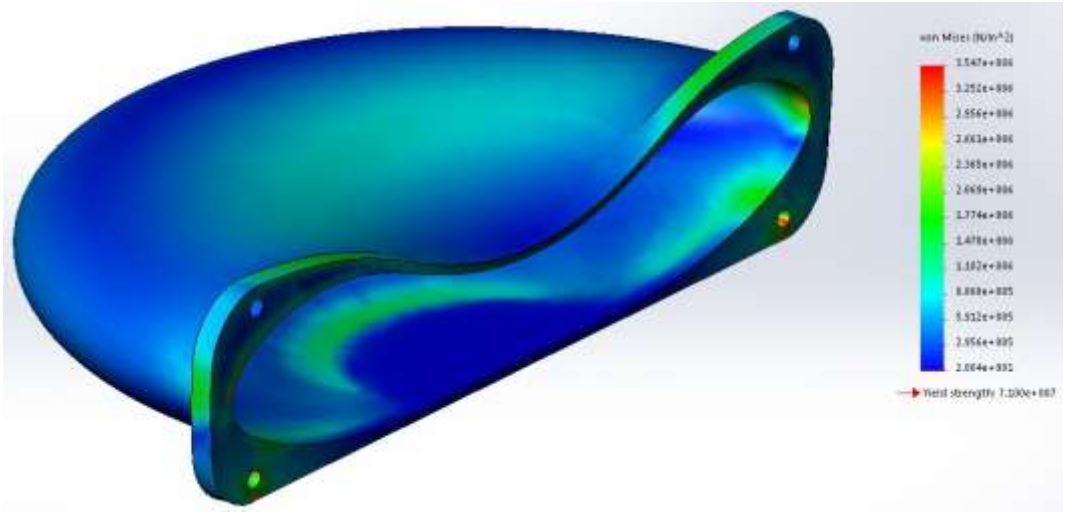

Figure 49: Skin layer component compression simulation

Mechanical properties of the cured epoxy resin mixture were derived from the data sheet on the constituents [31] and are assembled into Table 8.

Table 8: Mechanical properties of epoxy resin material

Parameter	Value
Density	981 kg/m^3
Young's modulus	2.11 GPa
Ultimate strength (tensile)	72.4 MPa
Poisson's ratio	0.35

Figure 50Figure 53 show results of compression simulation for all adipose layer components and fibro-glandular component. Table 11 presents values of maximum stresses occurring in the casted components and also provides factor values, which can be used as a magnitude of safety margin.

Table 9: Maximum stress in casted components

Component	Value	Difference factor
1st adipose layer	10.5 MPa	6.89
2nd adipose layer	11.4 MPa	6.35
3rd adipose layer	9.7 MPa	7.46
Fibro-glandular component	0.28 MPa	258

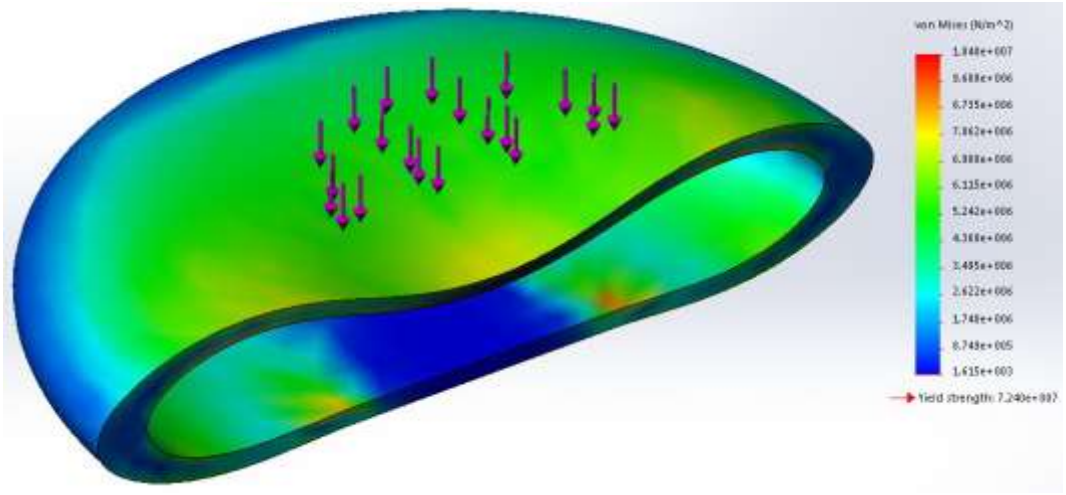

Figure 50: 1st adipose layer compression simulation

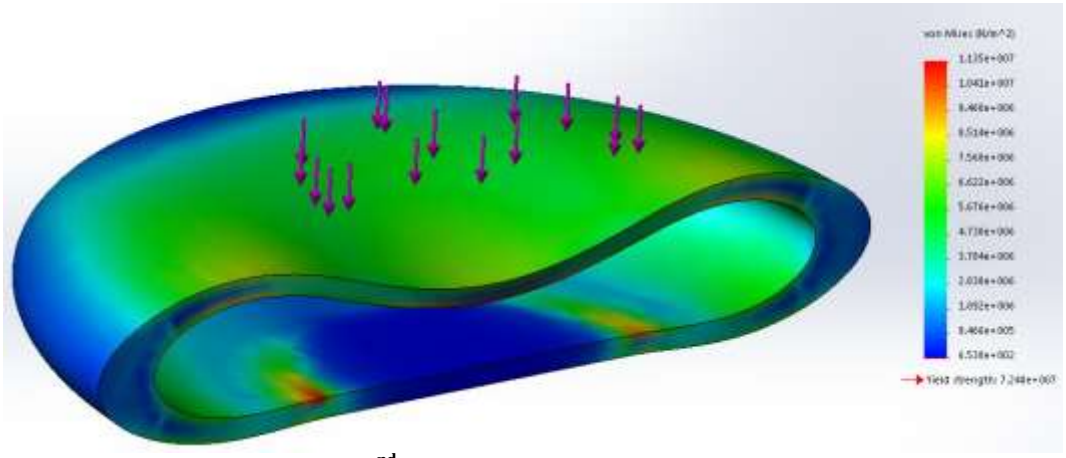

Figure 51: 2nd adipose layer compression simulation

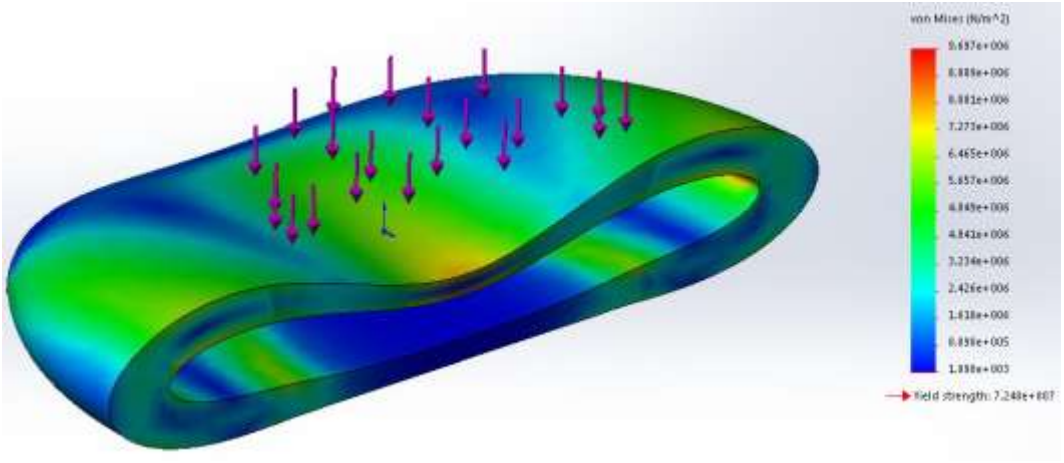

Figure 52: 3rd adipose layer compression simulation

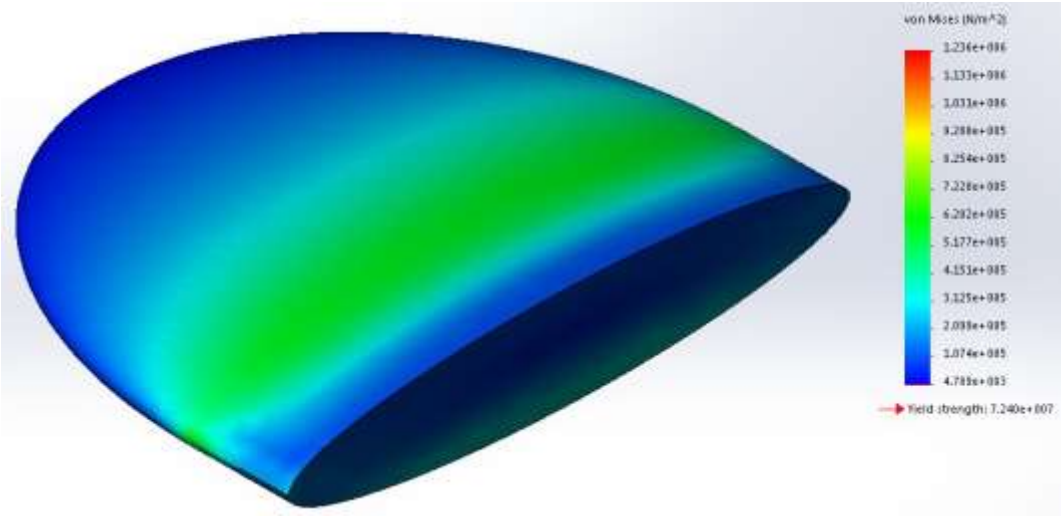

Figure 53: Fibroglandular component compression simulation

Chapter 5. Failure Mode and Effect Analysis

Failure Mode and Effect Analysis (FMEA) is usually performed to assess the risk involved in manufacturing and exploitation of the final product. In this case the term risk can be defined as follows:

Risk is an event, action or sequence of actions/events resulting in partial or complete malfunction of the object rendering it to be unable to perform its desired function.

The evaluation of potential risks provides ground for the creation of techniques and recommendations for prevention of these risks. Table 10 shows the grading which was used for the assessment of risks, which might occur during the fabrication and exploitation of the designed phantom.

Table 10: Grading of risk probability/severity

Rating	Probability	Severity
1	Very low (<20%)	Minimal
2	Low (20-39%)	Minor
3	Medium (40-59%)	Moderate
4	High (60-79%)	Significant
5	Very high (>80%)	Severe

Current FMEA is made for all three possible ways of manufacturing the final phantom and is assembled into Table 11.

Table 11: List of risk that might occur during manifacturing and exploitation of the designed phantom

Description	Prob.	Sev.	Total	Preventive measures	Contingent measures
Wrong composition of materials (epoxy resins)	1	5	5	Carefully measure and weigh the components	Repeat manufacturing
Wrong parameters for casting of the phantom	1	4	4	Simulate, model the casting process	Perform machining if possible; repeat casting procedure
Wrong dimensions due to thermosetting of 3D printing material	2	5	10	Test 3D printing materials and measure tolerances	Perform additional machining if possible
Damaged surface due to wrong parameters of CNC processing	1	4	4	Test CNC processing to acquire necessary parameters	Remove excessive material, patch insufficient regions repeat CNC processing
Damaged heterogeneity pattern (e.g. grooves, cavity) due to wrong moulding setup	1	4	4	Particular mould design for each moulding setup	Perform additional machining if possible
Damage of the phantom components due to wrong storage and handling	5	3	15	Introduce special procedures and instructions for storage and handling	If the damage is irreversible, order new components; provide spare parts
Wrong operation and handling by medical and technical personnel due to innovative design	5	1	5	Education and technical support of the personnel	Repeat previously performed procedures after adjusting for mistakes

Chapter 6. Future Developments

This chapter presents information on further work and possible development of the project to increase its performance and scientific and societal value. It discusses both design and manufacturing sides of the phantom, drawing conclusion to the project presented in the report.

Design development

The concept presented in the report has a big capacity for further improvement. The following features can be introduced into the future versions of the phantom:

- Simulation of more complex glandular structures
  The grooves present on the surface of the current version of the phantom can be manually changed in their shape, width and depth. One of the examples of complication of the structures is to use complex pitted 3D surface, which is later filled with glandular equivalent material.

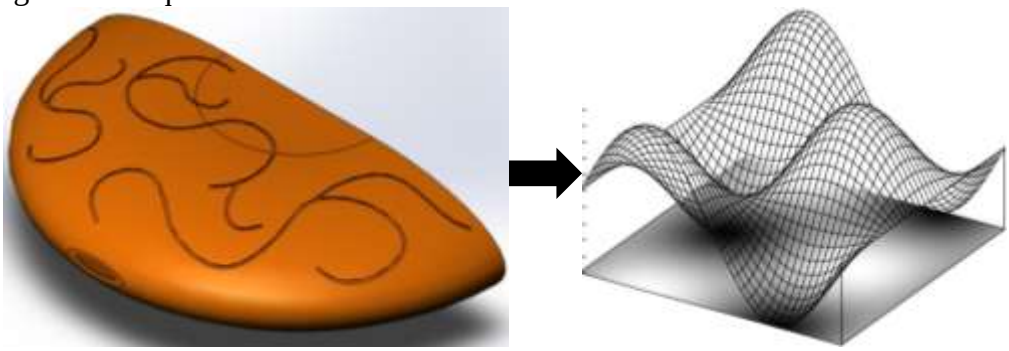

Figure 54: Complication of the surface from grooves to complex surface [32]

- Design of a complete set of features for image quality assessment and dosimetry
  The current design allows for a lot of room for inclusion of different features for image quality assessment. Therefore, next step would be a design of the complete set of such features, which can be introduced into the phantom components and easily assembled.

- Development of a specific software or a designing and manufacturing environment
  Additional advantage would be the creation of a specific software or environment in which a complete designing procedure can be done including complete simulation of complex and realistic breast anatomy, such as phantom shape, internal structure patterns, etc.

Manufacturing improvement

Although this project presents a short term solution for fast manufacturing of a phantom for the comparison of FFDM and DBT in a laboratory setup, there are certain characteristics that can be improved.

- Improved simulation of real breast by selection of more appropriate materials
  Current design can be improved to allow for using water as substance equivalent to glandular tissue. Certain amount of redesigning is necessary; however, the general structure of the phantom will remain unchanged.

- Complete 3D printing of the phantom
  Even though the report concludes that currently the phantom cannot be completely produced by 3D printing, further development of this technology together with an investigation of materials may result in a fast and easy manner to manufacture phantom.

Chapter 7. Ethics

Societal impact of the project

The goal of this project is to address the issue of comparing two imaging modalities for breast cancer detection: Full-Field Digital Mammography and Digital Breast Tomosynthesis. This comparison is to be performed by a specially designed phantom. The designed phantom will provide advantages to the current situation in healthcare and society, such as:

1. Provide means for both objective and subjective evaluation of performance of different systems for breast imaging. Future versions of this phantom can become a standard for FFDM and DBT accreditation resulting in better diagnostic accuracy of future breast imaging systems.
2. The new phantom may provide new ideas and approaches to resolving various problems of image reconstruction and removal of noise and artifacts from the acquired images. Certain research value of the phantom can be expected also.
3. The comparison and evaluation of the two modalities will result in the adoption of the optimal modality as a standard for breast cancer detection or combination of both modalities to provide better detection results at lower acceptable radiation exposure.

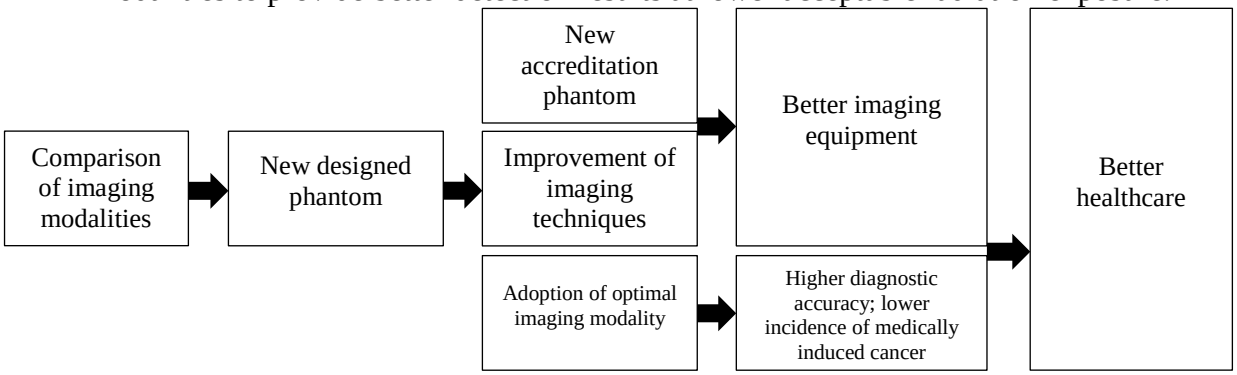

Figure 55: Diagram of societal impact of the project

Ethical characteristics of the project

This project has no conflicts of interest: it was performed independently of any companies or organizations whose equipment or resources were used or review in the course of the project.

Collaboration during this project had no restrictions imposed by any institution taking part in the project.

No patient data were specially obtained for this project, only those being anonymous, preliminary edited by third-party, and in open access were used for generating new ideas and early justification of concepts. Therefore no specific data protection measures were undertaken during project and no research restrictions associated with human or animal being research were necessary.

The author of this project takes upon himself the full responsibility for integrity of this project, acquisition and elaboration of any relevant data, and ensures that no misconducted research was performed in the course of the project.

Acknowledgements

This project would not be possible without consistent guidance of Alicja Daszczuk. She gladly provided me extensive assistance during the whole course of the project by answering my questions, giving new ideas, connecting me with people essential for further development of the project, and giving essential feedback.
Meetings with Dr. Marcel Greuter assured me that I was moving into the right direction. His always friendly yet objective reaction towards results of different stages of the project gave me additional motivation.
I would like to express my gratitude to my fellow student Niels van den Rheenen, whose collaboration resulted in fabrication of two prototypes. His knowledge of 3D printing was appropriate for my project and resulted in new ideas for future of the project.
General approach to the designing process taught by Prof. Bart Verkerke ensured thorough and multidirectional analysis of the design assignment and consequent designing stage.
This project would be incomplete without help of Folkje Bulthuis-Veenstra and Enouschka Schleurholts who offered their help in acquiring images of the prototype and materials for possible phantom manufacturing.

And of course I would like to thank my wife Ekaterina for all her patience while I was working on the thesis project. She made sure that I had enough time and proper working environment by taking my daughter Milana outside, when I needed some moments of concentration. Watching how Milana grows and persistently develops gave me new strength push the project forward and even a little bit further.

Bibliography

1. Boyd NF, Martin LJ, Bronskill M, Yaffe MJ, Duric N, Minkin S. Breast tissue composition and susceptibility to breast cancer. J Natl Cancer Inst. 2010;102(16):1224-37.
2. McCormack VA, Dos Santos Silva I. Breast density and parenchymal patterns as markers of breast cancer risk: a meta-analysis. Cancer Epidemiol Biomarkers Prev. 2006;15(6):1159-69.
3. DeSantis C, Ma J, Bryan L, Jemal A. Breast cancer statistics, 2013. CA Cancer J Clin. 2014;64(1):52-62.
4. Youlden DR, Cramb SM, Yip CH, Baade PD. Incidence and mortality of female breast cancer in the Asia-Pacific region. Cancer Biol Med. 2014;11(2):101-15.
5. Screening for Breast Cancer: U.S. Preventive Services Task Force Recommendation Statement, U.S. Preventive Task Force, 2009
6. Drukteinis JS, Mooney BP, Flowers CI, Gatenby RA. Beyond mammography: new frontiers in breast cancer screening. Am J Med. 2013;126(6):472-9.
7. Weinstein SP, Localio AR, Conant EF, Rosen M, Thomas KM, Schnall MD. Multimodality screening of high-risk women: a prospective cohort study. J Clin Oncol. 2009;27(36):6124-8.
8. Othman E, Wang J, Sprague BL, et al. Comparison of false positive rates for screening breast magnetic resonance imaging (MRI) in high risk women performed on stacked versus alternating schedules. Springerplus. 2015;4:77.
9. Andersson I, Ikeda DM, Zackrisson S, et al. Breast tomosynthesis and digital mammography: a comparison of breast cancer visibility and BIRADS classification in a population of cancers with subtle mammographic findings. Eur Radiol. 2008;18(12):2817-25.
10. Skaane P, Bandos AI, Gullien R, et al. Prospective trial comparing full-field digital mammography (FFDM) versus combined FFDM and tomosynthesis in a population-based screening programme using independent double reading with arbitration. Eur Radiol. 2013;23(8):2061-71.
11. Schulz-Wendtland R, Wenkel E, Lell M, Böhner C, Bautz WA, Mertelmeier T. Experimental phantom lesion detectability study using a digital breast tomosynthesis prototype system. Rofo. 2006;178(12):1219-23.
12. Brunner CC, Acciavatti RJ, Bakic PR, Maidment ADA, Williams MB, Kaczmarek R, Chakrabati K, Evaluation of Various Mammography Phantoms for Image Quality Assessment in Digital Breast Tomosynthesis: IWDM 2012, LNCS 7361. 2012: 284–291.
13. CIRS BR3D phantom information: http://www.cirsinc.com/products/all/51/br3d-breast-imaging-phantom/
14. Gammex Inc.: http://www.gammex.com/n-portfolio/productpage.asp?id=299&category=Mammography&name=Mammographic+Accreditation+Phantom%2C+Gammex+156
15. Carton AK, Bakic P, Ullberg C, Derand H, Maidment AD. Development of a physical 3D anthropomorphic breast phantom. Med Phys. 2011;38(2):891-6.
16. De las Heras H, Schoefer F, Weinheimer O, Semturs F, Chevalier M, Performance test of digital breast tomosynthesis using a dedicated phantom. Poster. ECR 2014.
17. Yaffe M. J., Boone J. M., Packard N., Alonzo-Proulx O., Huang S. -Y., Peressotti C. L., Al-Mayah A., and Brock K., The myth of the 50–50 breast, Med. Phys. 2009; 36: 5437–5443.
18. Feng SS, Patel B, Sechopoulos I. Objective models of compressed breast shapes undergoing mammography. Med Phys. 2013;40(3):031902.

19. Pope TL, Read ME, Medsker T, Buschi AJ, Brenbridge AN. Breast skin thickness: normal range and causes of thickening shown on film-screen mammography. J Can Assoc Radiol. 1984;35(4):365-8.
20. Van den Rheenen N. 3D phantom printing. Master Thesis. University of Groningen 2015.
21. Skrzyński W, Fabiszewska E, Tissue-equivalence of selected materials in mammography [Poster]
22. Zalewski M, Guerrilla guide to CNC machining, mold making, and resin casting, Chapter 4: http://lcamtuf.coredump.cx/gcnc/ch4/
23. Argo WP, Hintenlang K, Hintenlang DE. A tissue-equivalent phantom series for mammography dosimetry. J Appl Clin Med Phys. 2004;5(4):112-9.
24. Compton BG, Lewis JA. 3D-printing of lightweight cellular composites. Adv Mater Weinheim. 2014;26(34):5930-5.
25. Poletti ME, Goncalves OD, Mazzaro I. Measurements of X-ray scatter signatures for some tissue-equivalent materials. Nucl. Instr. and Meth. in Phys. Res. 2004;213(B): 595‑8.
26. Bouwman RW, Diaz O, Van engen RE, et al. Phantoms for quality control procedures in digital breast tomosynthesis: dose assessment. Phys Med Biol. 2013;58(13):4423-38.
27. Poletti ME, Gonçalves D, Mazzaro I. X-ray scattering from human breast tissues and breast-equivalent materials. Phys Med Biol. 2002;47(1):47-63.
28. Geraldelli W, Tomal A, Poletti ME. Characterization of Tissue-Equivalent Materials Through Measurements of the Linear Attenuation Coefficient and Scattering Profiles Obtained With Polyenergetic Beams. IEEE Trans. Nucl. Sc. 2013;60(2): 566-71.
29. Vollmar SV, Langner O, Weigel M, Bosmans H, Kalender WA. Breast phantom design for dedicated breast CT and breast tomosynthesis. IFMBE Proc. 2009;25/II: 53-6.
30. Prionas ND, Burkett GW, Mckenney SE, Chen L, Stern RL, Boone JM. Development of a patient-specific two-compartment anthropomorphic breast phantom. Phys Med Biol. 2012;57(13):4293-307.
31. Epoxy Formulations using JEFFAMINE® polyetheramines, Huntsman 2005.
32. Image: https://www.packtpub.com/sites/default/files/Article-Images/7249_08_12.png